Nuclear Engineering and Design 448 (2026) 114692

Contents lists available at ScienceDirect

Nuclear Engineering and Design

journal homepage: www.elsevier.com/locate/nucengdes

A CO_2-based real options model for assessing the impact of external events on nuclear power plants

Alessandro Paravano, Giacomo Galeotti, Alessandra Neri, Enrico Cagno, Giorgio Locatelli *

Politecnico di Milano, Piazza Leonardo da Vinci 32, 20133 Milan, Italy

ARTICLE INFO

Keywords:
Nuclear resilience
Risk modelling
Climate impact
CO_2 mitigation
Infrastructure
Decision tools
Megaprojects

ABSTRACT

Nuclear power plants (NPPs) are essential for decarbonization. However, external events such as prolonged droughts or earthquakes have historically compromised NPPs' availability, undermining their decarbonization potential in national energy mixes. Life Cycle Assessment (LCA) is widely used to evaluate the CO_2e savings of NPPs, yet it typically assumes ideal operating conditions and fails to account for external events. Conversely, models that account for external events mainly adopt Real Options Analysis (ROA). Historically, ROA focuses solely on economic implications and considers monetary indicators (e.g., the price of electricity) while overlooking the impact on CO_2e savings. No ROA study has examined the impact of external events on NPPs from a CO_2e perspective. Yet, such external events are crucial, as empirically demonstrated by the reduced capacity factor of French reactors due to prolonged droughts. In response, we develop a novel model to assess the impact of external events on NPPs' electricity production from a CO_2e perspective. We developed and tested the model through a pseudo-real case study focused on drought events and their effects on NPPs' cooling systems. The model has three key novelties: 1) it consists of an enhanced LCA that incorporates the impact of external events on the NPP LCA; 2) it introduces a ROA approach based on CO_2e emissions as the evaluation metric instead of money; 3) it incorporates uncertainty by considering multiple CO_2e emissions scenarios simultaneously in the case of droughts impacting NPPs.

1. Introduction

With life-cycle emissions as low as 12 gCO_2e/kWh (World Nuclear Association, 2024a), nuclear energy remains a cornerstone for decarbonizing electricity systems (Marcel, 2023; Adamov et al., 2025). In 2023, nuclear power plants (NPPs) generated approximately 2602 TWh of electricity, accounting for about 9 % of global electricity production (World Nuclear Association, 2024b). Over 70 GW of new nuclear capacity is under construction globally, marking one of the highest levels in the past three decades (IEA, 2025). To meet net-zero emissions targets by 2050, more than 30 countries have committed to tripling nuclear capacity, recognizing its role in providing reliable, low-carbon energy (Declaration to Triple Nuclear Energy, 2023.).

Yet NPPs remain vulnerable to various external events that can severely compromise their CO_2e savings potential in national energy mixes. Occurrences such as referendums or natural events have repeatedly compromised the expected contribution of NPPs to national energy systems. For instance, France has faced unexpected outages due to stress corrosion cracking in key reactor components or jellyfish blocking cooling filters. Such external events represent risks for NPPs, which are particularly relevant for decision-makers, especially from a CO_2e perspective, given that NPPs involve substantial upfront CO_2e expenditures, have long life-cycles, and rely on extended operational periods to deliver meaningful carbon returns. Prematurely shutting down or reducing availability hinders the CO_2e expected reductions.

Given the critical importance of CO_2e emissions in evaluating NPPs, the literature has extensively developed Life Cycle Assessment (LCA) models (Pucciarelli et al., 2024). Decision makers widely use LCA models to assess the net environmental benefit of NPPs by accounting for emissions across the entire life cycle (Frapin et al., 2022; Aminsharei et al., 2024), from uranium mining and plant construction to operation and decommissioning (Kirk et al., 2025). Studies consistently show that NPPs have significantly lower life-cycle emissions compared to fossil fuel-based plants (Poinssot et al., 2016), and, in some cases, are comparable to or even lower than renewable sources such as wind or solar (Wang et al., 2019). However, traditional LCA approaches rely on

* Corresponding author.
E-mail addresses: alessandro.paravano@polimi.it (A. Paravano), giacomo.galeotti@mail.polimi.it (G. Galeotti), alessandra.neri@polimi.it (A. Neri), enrico.cagno@polimi.it (E. Cagno), giorgio.locatelli@polimi.it (G. Locatelli).

https://doi.org/10.1016/j.nucengdes.2025.114692
Received 16 June 2025; Received in revised form 29 October 2025; Accepted 14 December 2025
Available online 21 December 2025

average operating conditions and standard project lifespans (Bauer et al., 2015), typically assuming uninterrupted performance and full capacity utilization (Nock and Baker, 2019). This leads to the first literature limitation addressed in our paper: LCA models often fail to incorporate the impact of risks, such as external events, on the actual performance and carbon footprint of NPPs. As a result, the environmental assessments might miscalculate the actual CO_2e savings of NPPs under real-world conditions.

Recent literature has introduced integrated risk management processes to account for the impact of external events on NPPs' life-cycle. They support the coordination of project quality, cost, and scheduling (IAEA, 2023) and promote flexible and modular NPP systems design and development, e.g., load-following capabilities (Locatelli et al., 2015) or thermal energy storage integration (Faizan et al., 2024), to anticipate and mitigate the future external events' impacts on NPPs (de Neufville and Scholtes, 2011). Investment in flexible NPP systems is evaluated using Real Options Analysis (ROA) models, which embed uncertainties by assessing a broad spectrum of possible scenarios (Kodukula and Papudesu, 2006; Cardin et al., 2020). ROA model based on Monte Carlo Simulations (MCS) has been employed to account for a variety of uncertainties, including future revenues (Kiriyama and Suzuki, 2004), electricity prices (Jain et al., 2013), electricity demand (Cardin et al., 2017), social acceptance (Cardin et al., 2017), water prices (Arasteh, 2024), operation and maintenance costs (Locatelli et al., 2015), carbon credits (Kiriyama and Suzuki, 2004), and the evolution of the regulatory environment (Jeon, 2019). Regarding NPPs assessment, ROA has only been used from an economic perspective so far (Steer et al., 2012; Jain et al., 2013). This leads to the second limitation addressed in our paper: the literature does not account for CO_2e-related aspects in evaluating the impacts of external events on NPPs. For instance, the failure of key components can shorten the life of a NPP, leading not only to an economic damage, but also to a considerable reduction in low carbon electricity production. The opposite can also be true, e.g., life extension programs may prolong NPPs' operation beyond their originally expected lifespan.

To this end, our paper aims to develop a novel model for assessing the impact of external events on NPPs electricity production, incorporating risks in the NPPs' LCA (addressing limitation 1), and assessing their impact on CO_2e rather than money in the ROA (addressing limitation 2). The model is tested through a pseudo-real case study focused on drought risk and its impact on a 1000 MWe Pressurized Water Reactor (PWR), in Caorso on the Po River, Italy. We evaluate the option of building a water reserve to mitigate the impact of drought scenarios.

Without such a model, it is hard to establish whether building a water reserve is beneficial, especially concerning CO_2e emissions. We focus on drought risk as the reference external event to develop and demonstrate the proposed CO_2-based ROA model. This choice is motivated by both practical and methodological considerations. From a practical perspective, drought represents one of the most critical and recurrent environmental stressors for NPPs, particularly in Southern Europe, where water availability plays a key role in cooling processes and plant efficiency. The increasing frequency and severity of droughts due to climate change make this phenomenon a relevant and timely case for analysis. From a methodological standpoint, drought provides a well-documented and quantifiable example that enables transparent modelling based on publicly accessible data. Crucially, the focus on drought should not be interpreted as a limitation of scope, but rather as a demonstration to showcase the flexibility and applicability of the proposed framework.

The results have relevant implications for both theory and practice. The model opens new avenues for integrating risk and sustainability assessments in NPPs appraisal. The model provides a decision-support tool capable of informing investments and policy choices under uncertain conditions, focusing on long-term CO_2 mitigation outcomes that complement economic analysis. This is especially relevant in climate adaptation, where traditional metrics may underestimate the environmental costs of operational disruptions. It also extends the scope of LCA by embedding operational uncertainties, offering a more realistic basis for environmental performance evaluation.

The rest of the paper is structured as follows. Section 2 focuses on the characterization and modelling of drought risk and its potential impact on an NPP operations. Section 3 details the model, outlining its key assumptions, mathematical formulation, and methodological setup. Section 4 applies the model to a pseudo-real case study, illustrating the implementation and analyzing the results across multiple drought scenarios. Finally, Section 5 discusses the main conclusions, implications, limitations and future research.

2. Drought risk for NPPs

2.1. Drought risk index

Drought is an exceptional period of water shortage for existing ecosystems and the human population (due to low rainfall, high temperature and/or wind) (IPCC, 2021). Drought risk is the risk of unmet energy demand due to drought (Rossi et al., 2023). NPP drought-induced losses are projected to increase due to greater variability in precipitation and higher potential evaporation driven by increased warming (Rossi et al., 2023). European plants, particularly in the South of France, and potentially in Italy, could see the most significant percentage increases in consecutive dry days (Raso et al., 2019). This risk is particularly significant for power plants cooled with water from rivers and lakes, unlike those situated by the sea or ocean, which have access to abundant and potentially limitless water supplies. France, for example, has multiple NPPs along rivers and faced substantial challenges during the 2003 drought. French NPPs had to reduce output to comply with regulations concerning river water temperatures, resulting in a total energy loss of 3.3 TWh between July and August 2003 (IAEA, 2004). In the summer of 2024, the Golfech NPP in southwestern France had to reduce its output by around 1 GW after rising water temperatures in the Garonne River exceeded regulatory limits for cooling water use, according to Électricité de France (EDF) and Reuters reports (Crellin, 2024). Similarly, the drought severely impacted Italy's Po River (that cooled one of the old Italian reactors), where hydrological data show the annual average flow dropped to 610 m^3/s from the usual 1,000–1,100 m^3/s (Mombrini et al., 2025). In 2022, another intense drought forced several thermal power plants in Italy to shut down during the summer (Giliberto, 2022; Ramírez Molina et al., 2024). These events underscore the importance of incorporating drought considerations into NPPs' future energy production.

The Standardized Precipitation Index (SPI) is widely used to measure drought severity. As a z-score, the SPI indicates how much current precipitation deviates from historical averages, with negative values representing drier-than-average conditions and positive values indicating wetter conditions (Scarsini et al., 2024; EDO, 2025), focusing on the uncertainty inherent in drought events. The confidence intervals can vary significantly, while average SPI values remain largely consistent, whether or not uncertainty is considered (Liu et al., 2014). In this study, we utilize the Streamflow Drought Index (SDI), which provides a direct and standardized measure of hydrological drought conditions based on actual river flow data (see Appendix), allowing for consistent monitoring and comparison across different time scales and regions under uncertainty (Nalbantis and Tsakiris, 2009).

The construction of surface reservoirs is a reasonable solution for increasing the NPP water supply, reducing the risk of drought (Rossi, 2000). The IAEA report presents the Palo Verde Nuclear Generating Station as an exemplary case study of resilience and reliability within the nuclear industry (IAEA, 2022). Palo Verde is located in Arizona, USA, in the middle of a desert, far from any natural water bodies (Redfoot et al., 2022). The plant obtains all its cooling water from the Phoenix 91st Avenue wastewater treatment facility via a 60 km combined gravity flow and pumped pipeline system (IAEA, 2012). Upon arrival, the water undergoes further treatment at the on-site water reclamation facility (Middleton et al., 2021) and is then pumped into adjacent reservoirs. Palo Verde has two reservoirs, which provide a total of 4.4 million m^3 of treated water storage. Both reservoirs are lined with 60 mm-thick inner and outer high-density polyethene and a netting layer in between, with the liners having an expected lifespan of 20 years (Peachey, 2013).

2.2. River flow forecasting

Recent literature on short- and long-term daily river flow forecasting predominantly focuses on Artificial Neural Networks (ANN) (Samui et al., 2023). In long-term forecasting, the models analyzed typically predict only a few years (Niu et al., 2018) and often lack uncertainty analysis (Noorbeh et al., 2020). Additionally, these models do not generate multiple simulations due to the deterministic nature of ANN results (Li et al., 2019). Only Riahi-Madvar et al. (2021) employs a “long-term” MCS alongside ANNs, offering a one-year forecast and generating 90 simulations (Riahi-Madvar et al., 2021). MCS accounts for and quantifies uncertainties in river flow forecasting models by generating multiple simulated outcomes through varying input parameters (lags of antecedent river flows) and model structures, thereby providing an uncertainty analysis of the predictions. Some studies adopt preprocessing techniques from signal analysis theory (Li et al., 2019; Zhang et al., 2022) to remove noise while preserving the time dependency of data, thus accounting for flow patterns. One such modern technique is Discrete Wavelet Transform (DWT) analysis (Russell et al., 2020), which preprocesses data fed into neural networks, producing highly reliable results. While DWT could serve as a superior pattern recognition tool when combined with MCS, possibly even outperforming the method used in the present work, it is traditionally applied in the context of deterministic ANNs and signal processing in the literature.

3. Methodology

The ROA model is developed and tested to evaluate the option of building a small backup water reservoir close to the NPP located near the Po River to mitigate drought risk (see Section 4.2.1 for the reservoir details). By making this preliminary investment, the plant gains increased flexibility; specifically, the decision-maker secures the option to expand the water reservoir, potentially enlarging it up to 40 times its original size and mitigating the risk of droughts. The methodology to develop the ROA model consists of three phases (Fig. 1):

1) Model setup. In the first phase (Section 3.2), we compute the option price, the exercise price, and additional operational costs in terms of CO_2e and conduct the necessary preliminary river flow analysis.
2) Model simulation. In the second phase (Section 3.3), we perform MCS to forecast future river flows, estimate the NPP future power generation, and calculate the associated emissions savings. These calculations are performed for the following scenarios: a) with the investment in the reservoir and b) without the investment to effectively quantify the impact of the reservoir.
3) NPV_{CO2e} calculation and suggestions to decision-makers. Finally, we calculate the NPV_{CO2e} of the reservoir building using CO_2e as a decision metric (Section 4). We analyse the results through a sensitivity analysis and perform a threshold analysis (Locatelli et al., 2020) to provide recommendations to decision-makers.

The model introduces three key methodological innovations. First, it enhances the traditional NPPs’ LCA by integrating the consequences of external events, such as drought-induced reductions in cooling water availability, which can significantly constrain the NPP electricity production during its operation. This allows the model to accurately reflect real-world deviations from expected energy production. Second, it shifts the ROA focus from monetary metrics to CO_2e emissions, enabling decision-makers to assess the value of operational flexibility or mitigation investments in environmental terms. Third, the model incorporates uncertainty by simulating multiple drought scenarios associated with reduced NPP electricity production patterns and CO_2e performance. This probabilistic approach captures a broader range of possible environmental outcomes, moving beyond average-case assumptions and allowing for more informed, resilience-oriented planning.

3.1. Inputs, hypotheses, and assumptions

3.1.1. Input parameters

We focus on drought risk as an exemplary external event to develop and test the proposed model. This choice is motivated by several considerations. First, droughts represent one of the most relevant and increasingly frequent environmental risks affecting NPPs, particularly in Southern Europe, where water scarcity can directly constrain cooling capacity and, consequently, plant performance and operational reliability. Second, droughts are characterized by well-documented statistical patterns and widely available reported data, which allows for transparent parameterization, facilitating model validation and reproducibility. Third, by selecting drought, we aim to demonstrate the methodological value and flexibility of the proposed CO_2-based real options model. The approach can be generalized to other types of external risks, such as seismic risks or grid reliability risks, thus illustrating how uncertainty and environmental variability can be systematically incorporated into energy infrastructure life cycle–based decision analyses.

The input parameters for the model are organized according to the phase in which they are required (Table 1), described below in detail. All setup inputs are utilized during the simulation phase to evaluate the real option. Design choice parameters are specific to the location of the NPP; they are necessary for the model, but their specific values do not significantly affect the overall results. We chose Caorso, in the North of Italy, as the location for this study because it is the site of the only NPP ever built on the Po River, namely the Caorso NPP, the biggest ever built in Italy, which is currently being decommissioned. Data on the Caorso NPP is publicly available at Regional Agency for Prevention, Environment and Energy of Emilia-Romagna website (ARPAE-SIMC, 2024) The data used in this work covers the following periods and locations:

- Historical average daily flow values [m^3/s] from the Piacenza Hydrological Station from 1960 to 2020.
- Historical average water temperature [°C] from the Piacenza hydrological station from 2000 to 2023.
- Historical average daily air temperature [°C] from the Piacenza station from 2004 to 2023.
- Historical average daily relative humidity [%] from the Piacenza station from 2013 to 2023.
- Italian average yearly carbon intensity (CI) values are taken for the period 1990–2023.

The parameters originate from a combination of vendor data (Sogin Spa, 2025), literature-based references, and design or simulation assumptions, depending on their role in the model. Plant ratings and efficiencies are based on standard vendor nameplate values for an APR1000 reactor (1,000 MWe, 37 % efficiency) and are used solely to determine system flows and loads. These parameters provide realistic operational scales but do not influence the calibration of the results. The average water consumption of 0.7 m^3/s at full power is derived from the IAEA WAMP dataset, which represents a consistent basis for converting hydrological inputs (e.g., river discharge, weather) into cooling water requirements (IAEA, 2018). The plant design life is set to 60 years, reflecting the expected operational lifetime of modern nuclear power plants and aligning with current vendor technical documentation. The low-flow threshold (270 m^3/s in the base case) represents the “Severe drought” category according to the SDI and is varied between 200 and

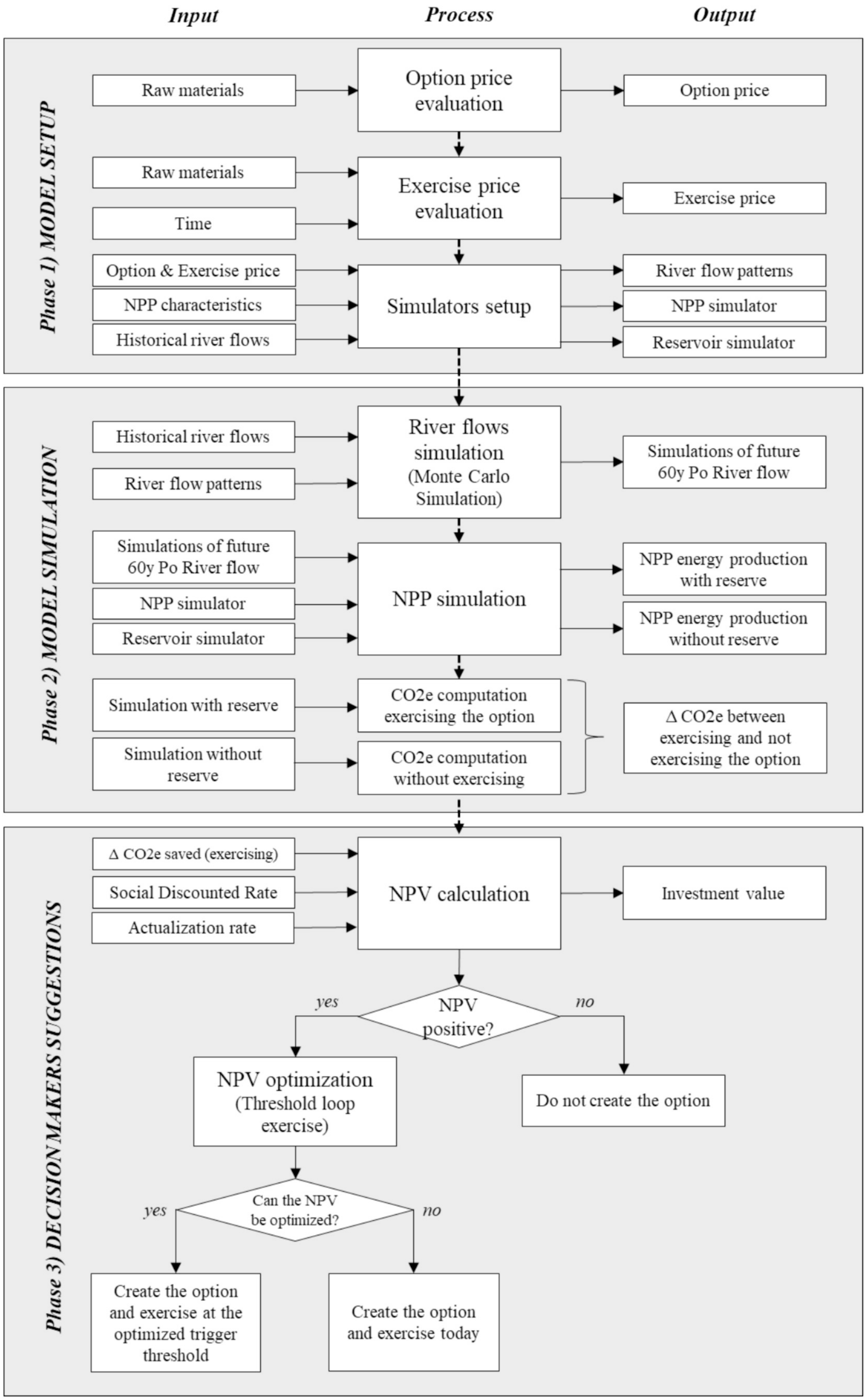

Fig. 1. Model logical flow.

Table 1
Summary of parameters and values used in the model setup and simulation phase.

Purpose	Parameter	Value	Unit Measure	Source
Reserve Size	Power Plant Output	1000	MWe	(Hydro and Corporation, 2019)
Reserve Size	Plant Efficiency	37	%	(Hydro and Corporation, 2019)
Reserve Size	Avg. Water Consumption	0.7	m^3/s	(IAEA, 2018)
Option Costs	Concrete Emissions	0.275	$tonCO_2/ton$	(IPCC, WMO, and UNEP, 2022)
Option Costs	Steel Emissions	1.83	$tonCO_2/ton$	(IPCC, WMO, and UNEP, 2022)
Option Costs	Backup Basin Dimension	0.5	days of consumption	Assumption
Option Costs	Basin depth	6	M	Assumption
Option Costs	Reservoir Dimension	6	days of consumption	Assumption
Option Costs	HDPE Unitary Emissions	0–16,000	$tonCO_2$/ tonHDPE	(ERG Franklin Associates, 2020)
Option Costs	HDPE Density	950	kg/m^3	(ERG Franklin Associates, 2020)
Option Costs	HDPE Liner Thickness	60	Mm	(Peachey, 2013)
Option Costs	Liners Number	2	#	(Peachey, 2013)
Option Costs	Reserve Construction Time	1	Year	Assumption
Option Costs	Italian Carbon Intensity	dataset	%	(Global Carbon Budget, 2025)
Simulations	Plant Design Life	60	Years	(Hydro and Corporation, 2019)
Simulations	Live Steam Temperature	294	C	(Hydro and Corporation, 2019)
Simulations	Condenser Approach	6	C	Assumption
Simulations	Condenser Range	10	C	Assumption
Simulations	Cooling Tower Approach	6	C	Assumption
Simulations	Cycles of Concentration	6	#	Assumption
Simulations	Flow Values	Dataset	m^3/s	(ARPAE, 2024)
Simulations	Water Temperature	Dataset	C	(ARPAE, 2024)
Simulations	Air Temperature	Dataset	C	(ARPAE, 2024)
Simulations	Air Relative Humidity	Dataset	%	(ARPAE, 2024)

340 m^3/s in sensitivity analysis. This range captures different interpretations of ecological protection and water management policies. We assumed a maximum water withdrawal rate between 0.0001 % and 1 % of the daily river flow, and its impact was evaluated through a sensitivity analysis described in Section 4.2. The corresponding reserve size (0.9 million m^3) and depth are scaled from the Palo Verde nuclear station's twin-reservoir system to a single-unit European configuration. This design choice ensures consistency with proven engineering precedents while maintaining realistic operational autonomy (approximately 15 days of full-power cooling). The option price of 25,000 tCO_2e represents the embodied carbon associated with constructing the additional reinforced concrete and steel infrastructure required to "pre-enable" the reservoir connection. This estimate is derived from a conservative parametric scaling of comparable civil works, such as reinforced-concrete cooling towers, and is primarily used to evaluate the trade-off between construction-related emissions and operational CO_2e benefits. Since no previous LCA studies exist for this enabling infrastructure, we adopted a "cooling-tower-equivalent" surrogate approach to estimate the embodied carbon of the additional reinforced concrete and steel required. Mechanical-draft cooling towers are field-erected reinforced-concrete and steel structures supporting fan decks, basins, and piping systems (Bureau of Energy Efficiency, 2004). Typical multi-cell configurations for power-plant duty handle flow rates in tens of thousands m^3/h and use materials of similar density and composition to heavy civil works in nuclear balance-of-plant construction. Applying standard emission factors, 350–400 $kgCO_2e/m^3$ for reinforced concrete and 1.9–2.2 tCO_2e/t for structural steel, to the material quantities implied by these tower-scale systems yields an embodied carbon of roughly 10,000 tCO_2e. Since the enabling works considered in this study also include larger civil components such as pump bays, intake galleries, pipe racks, valve manifolds, and foundation tie-ins, we applied a conservative scaling factor of 2–3×, resulting in a central estimate of 25,000 tCO_2e, with a sensitivity range between 0 and 50,000 tCO_2e. To test the robustness of this approximation, a sensitivity analysis was performed by varying the option price across this range. Sensitivity analyses show that variations in this parameter have a limited effect on the overall NPV_{CO2e} compared to operational factors such as hydrology or maintenance. The High-Density Polyethylene (HDPE) liner configuration (two layers, 60 mm each) directly mirrors Palo Verde's engineering design, ensuring mechanical robustness and environmental protection. Given the variability of life-cycle emissions for HDPE, we adopted a wide sensitivity range (0–16 tCO_2e/t) based on comprehensive LCA studies to capture different resin compositions and boundary conditions. Parameters related to thermodynamic design (e.g., condenser approach and range, cooling tower characteristics, and cycles of concentration) are treated as design choices aimed at ensuring realistic plant behavior and operational flexibility under different environmental conditions. The meteorological and hydrological data (flow, water temperature, air temperature, and relative humidity) are sourced from ARPAE's open datasets for the Emilia-Romagna region, specifically from the Castellazzo Villanova d'Arda station near the Caorso site. These real historical series (2004–2024) ensure that the simulations reflect local climatic variability and realistic operating conditions (ARPAE SIMC, 2024).

3.1.2. River water consumption and regulation hypotheses

Power plant water usage is regulated by law to protect natural water bodies from adverse impacts. In Italy, the Merli Law (Italian Government, 2006) focuses explicitly on limiting the thermal impact of industrial activities on natural water bodies. This law restricts the temperature of industrial effluents discharged into water bodies, setting a maximum of 35 °C to safeguard aquatic ecosystems from the harmful effects of artificial temperature changes. Considering this regulatory background, the implications are:

- Maximum water withdrawal: the power plant's water intake is limited to between 0.1% and 1% of the daily river flow. For example, if the daily average river flow is 1,500 m^3/s, the power plant can withdraw a maximum of 15 m^3/s over a day (15 m^3/s × 86,400 s/day).
- Low-flow level restrictions: when the daily river discharge falls below the level corresponding to "severe drought" defined by the SDI (see Table A1 in Appendix). Water withdrawal from the river is no longer permitted. This critical river level is referred to as the "low-flow level".

The primary reason for implementing these additional constraints is to adopt a long-term perspective on the model. To assess the impact of these assumptions, we perform a sensitivity analysis (Section 4).

3.1.3. River flow hypothesis

To realistically model future river flow values using an MCS, we assume that future river flow patterns will align with historical patterns. This assumption enables the MCS to organize sampled values according to historical sequences (ranks), resulting in simulations that reflect realistic temporal variability. The strength of this assumption lies in its flexibility; it can be applied regardless of the probability distribution used in the MCS. Since this approach focuses solely on the relative ordering of values among themselves and between past and future datasets, it preserves the temporal patterns inherent in the historical data while allowing for variability in the magnitude of river flows. This method ensures that the simulations maintain realistic flow sequences, which is crucial for accurately modelling the operational and environmental impacts on the power plant.

3.2. Step 1: model setup

In the setup phase, we conduct preliminary analyses and computations that lay the groundwork for the simulation phase. These analyses involve calculating the option and exercise prices, estimating future ranges of CO_2e values, determining the operational costs associated with exercising the option, and extrapolating river flow patterns.

3.2.1. Option price and exercise price

The option price represents the amount of CO_2e emissions that the decision-makers incur when building a water reservoir. The exercise price is the amount of CO_2e emissions the decision-makers will incur if they exercise the option (using the reservoir). Fig. 2 presents the key metrics used to calculate the reserve volume, the area covered with HDPE, and the option price for constructing the basin with HDPE.

Due to the complexity of estimating this expenditure in terms of CO_2e emissions, we approximate the option price by calculating the CO_2e emissions per ton of steel and concrete (Table 1) and accounting for the material required for enhanced the NPP flexibility. We estimate it using the amount of reinforced concrete and steel required for a cooling tower, which is approximately 10,000 tons of CO_2e. A sensitivity analysis is then performed to assess the impact of this estimate on the results. The model introduces a new parameter for the reserve size, denoted as the total volume of the reserve: e_{wc} [m^3], which is used to compute the exercise price. This parameter represents the equivalent volume of water consumed by the NPP operating at full power for d days. Thus, if $d = 3$, it means that the reserve has enough water to supply the NPP at full power for three days. The Equation for e_{wc} is:

$$e_{wc} = w_c{*}d{*}24{*}3600 \tag{1}$$

where:

- w_c is the water consumption rate of the NPP at full power [m^3/s],
- d is the number of days the reserve should supply,

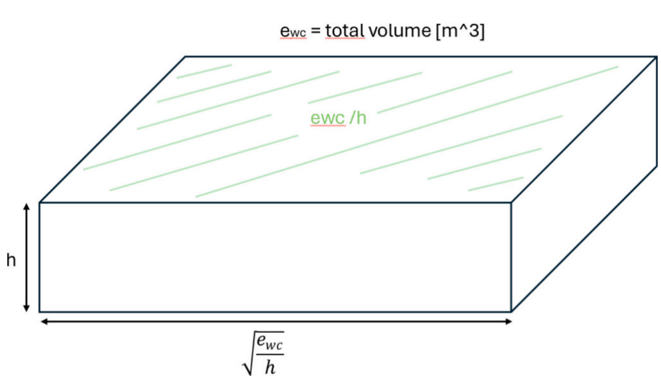

Fig. 2. Reservoir metrics.

- 24×3600 converts days to seconds.

Using the calculated value of e_{wc}, we determine the total covered surface area C_s [m^2] that the reservoir needs to be covered by HDPE liner. Eq. (2) accounts for the base area and the walls of a square-shaped reservoir, ensuring an accurate estimation of the HDPE lining required. The formula is:

$$C_s = \frac{e_{wc}}{h} + 4h\sqrt{\frac{e_{wc}}{h}} \tag{2}$$

where:

- h [m] is the height of the reserve.

Next, we compute the exercise price P_e [tons of CO_2e], which represents the additional CO_2e emissions associated with constructing the reservoir:

$$P_e = n_{liners} \bullet C_s \bullet l_t \bullet \rho \bullet CO_{2e(HDPE)} \tag{3}$$

where:

- C_s [m^2] is the total surface area to be lined, l_t [m] is the HDPE liner thickness;
- n_{liners} is the number of HDPE liners used to line the reserve;
- ρ [ton/m^3] is the density of HDPE;
- $CO_2e_{(HDPE)}$ [ton CO_2e/ton] is the unitary emissions of the HDPE material.

Due to challenges in finding precise literature values for $CO_2e_{(HDPE)}$, we perform a sensitivity analysis using values ranging from 0 to 16 tonCO_2e/ton, based on the cradle-to-gate study (ERG Franklin Associates, 2020). Building on the IPCC's concept of cumulative emissions (IPCC, 2021), we argue that preventing the release of 1 ton of CO_2e today is more valuable than delaying this action. Therefore, it is necessary to apply a discount rate to future emissions and savings, which is embedded in the inflation parameter WACCO_2e.

In the results section (Section 4), we present the exercise price plot (Fig. 13) illustrating how P_e is influenced by the two main variables in Eq. (3): the reserve height h and the pipes' HDPE unitary emissions $CO_2e_{(HDPE)}$. Fig. 13 shows a linear dependency of P_e on the HDPE emissions and an inverse exponential dependency on the reservoir height h. Increasing the reservoir height reduces the surface area C_s that needs to be lined, thereby decreasing the exercise price P_e.

3.2.2. Country and nuclear carbon intensity

Carbon intensity (CI) is defined as the amount of CO_2e per unit of energy produced (World Bank, 2024), commonly expressed in grams of CO_2e per kilowatt-hour ([gCO_2e/kWh]). In this work, we use CI to compute the emissions associated with the power generated during the forecasted period. These calculations are then utilized in the NPV_{CO2e} computation section to estimate the potential emissions savings from the NPP electricity production. The baseline is defined as a base-case CI trajectory, corresponding to Italy's historical average year-on-year reduction in grid CI. Best- and worst-case scenarios are constructed by adjusting this baseline by ±0.5 %. We analyse historical CI data from 1990 to 2023 to establish a baseline scenario. The average historical percentage change in CI is calculated and used as the base case. We adjust the base case for the worst-case and best-case scenarios by adding and subtracting 0.5 %. For the NPP, the CI is assumed to be 5 gCO_2e/kWh (UNECE, 2022). Fig. 3 illustrates Italy's historical CI (blue line) alongside the year-over-year delta change (purple line). The figure also includes projections based on three scenarios: the average annual decrease (base case), the most optimistic reduction trajectory (best case), and the least favorable outcome (worst case). These scenarios compare possible future trends in CI depending on different policies and

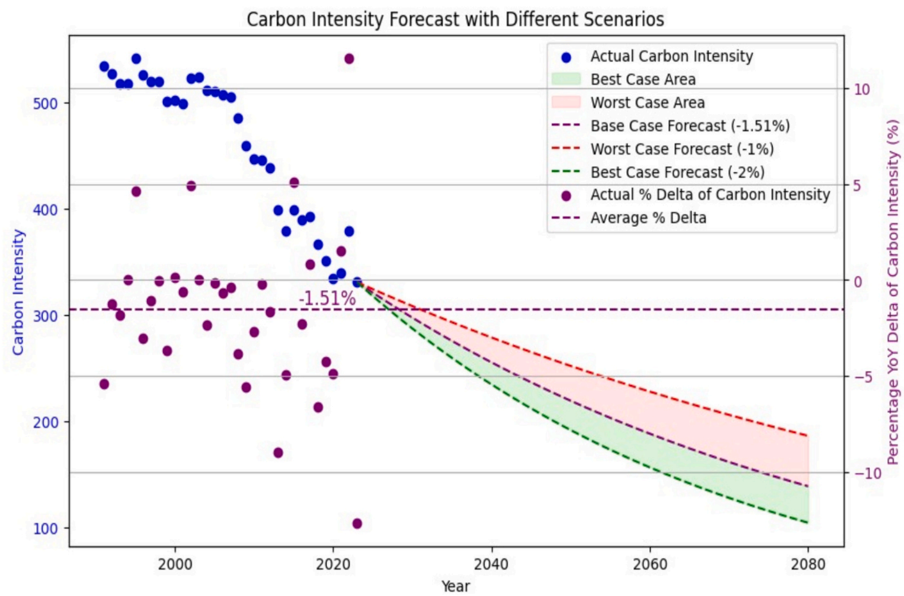

Fig. 3. Carbon intensity base, worst and best scenarios.

technological developments.

3.2.3. Operational CO_2e costs

The operational costs of the option are primarily attributed to the additional pump required to continuously supply water to the reserve, as the pump used to feed the NPP would be present in both cases. The power required by this pump is calculated using the following equations (Houghtalen et al., 2016):

$$P_{hydraulic} = \rho \cdot g \cdot Q \cdot H \quad (4)$$

$$P_{pump} = \frac{P_{hydraulic}}{\eta} \quad (5)$$

where:

- $P_{\mathrm{hydraulic}}$ [W] is the hydraulic power required to lift the water,
- ρ [kg/m^3] is the density of water,
- g [m/s^2] is the acceleration due to gravity (9.81 m/s^2),
- Q [m^3/s] is the pump's maximum flow rate,
- H [m] is the vertical elevation difference between the river and the reserve, and
- η is the efficiency of the pump. In the case of a 1.5 m^3/s pump (chosen in the case of the APR1000) MW$_e$ equations return around 1324.35 KW$_h$/day.

This translates into operating emissions (O_e) [tonCO_2e] given by:

$$O_e = \sum_{d=d_i}^{D_f} E_d \bullet CI(t) \quad (6)$$

where:

- E_d [kWh/day] is the daily energy consumed by the pump,
- d_i is the first day of operation,
- D_f is the last day of operation, and
- CI(t) [ton CO_2e/kWh] is the carbon intensity of the electricity grid in year t.

By summing the product of daily energy consumption and the corresponding CI over the entire period from d_i to D_f, the total operating emissions due to the pump's energy use are calculated, accounting for the temporal changes in CI.

3.2.4. Probability distributions and flow patterns

The standard distributions for river flow modelling include Log-normal, Weibull, and Gamma (Gupta and Waymire, 1990; Almeida et al., 2021; Durighetto et al., 2022). We employ the Kolmogorov-Smirnov test (Teegavarapu, 2019) and quantile-quantile plots to validate the goodness of fit for these distributions. These tools assist in determining the most suitable data windows for analysis, such as 10, 20, and 30-year periods. After assessing the fitness across different time windows, we selected 20 years fitted with a log-normal distribution function. Following the selection of appropriate probability distributions for each season, we projected future data distributions to incorporate changes in flow values into the model. Due to the limited number of data points, we apply linear regression to forecast future probability distributions. Although the Autoregressive Integrated Moving Average forecasting technique (Box et al., 2015) could offer more accurate results, it requires a larger dataset, which is not available in this study. Historical and forecasted probability distributions are in Fig. 4. Flow historical patterns are extracted based on the chosen time window for probability distribution selection.

3.2.5. Simulation parameters setup

The key parameters and their base case values are as follows (sensitivity analysis discussed in Section 4):

- Low-flow limit: the base-case value is set to 270 m^3/s, corresponding to a "Severe drought" SDI z-score probability of 4.4 %.
- Regulatory withdrawal limit: the regulatory parameter limiting maximum daily or monthly water withdrawal is set to 0.25 % as the base case value.
- Reserve size: the base-case reserve size is 0.9 million cubic meters of water, based on the re-scaled dimensions of the Palo Verde reserve.
- Reserve height: the base-case reserve height (depth) matches that of the Palo Verde reserve.
- Option price: following an initial estimation, the price is 25,000 tonCO_2.
- HDPE emissions: based on an incomplete cradle-to-gate LCA (ERG Franklin Associates, 2020), the HDPE unitary emissions are taken as the average value between 0 and 16 tonCO_2e/ton.
- WACCO_2e: 4 %.

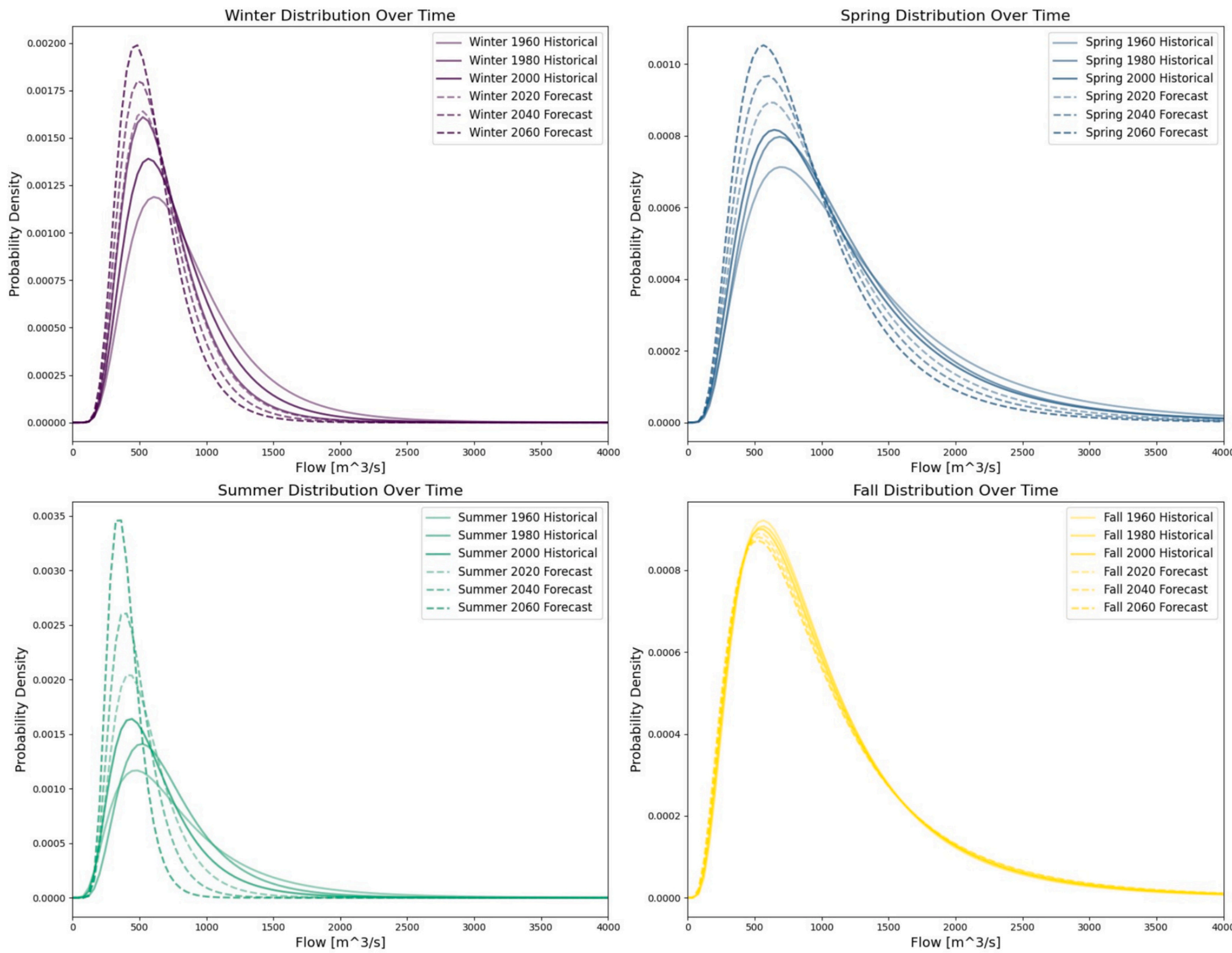

Fig. 4. Historical and Forecasted probability distributions of Po river flow.

- Inflation rate: 1.5 %.

3.3. Step 2: model simulations

The MCS is performed by sampling the probability distributions for each year and season. The sampled values are then rearranged according to a random pattern derived from historical flow patterns. Given the novelty of this MCS approach to river flow forecasting, it is essential to validate its consistency by simulating historical values and comparing them with actual flow data.

3.3.1. Water and NPP simulations

The IAEA's WAMP software (IEAE, 2018), adapted for this study to compute water withdrawal and consumption, requires daily flow values and additional weather data inputs, including river water and air temperatures, and relative humidity, to accurately predict the NPP's water needs. This complexity is simplified by applying standard average curves without accounting for the correlation between weather variables. Specifically, the standard applied curves are based on historical data. For relative humidity, we adopted the average values from the last 10 years, which is 75 %.

NPP simulators, both with and without reserves, are functions that use environmental and technical inputs (the forecasts) to output daily water consumption and power production over the NPP's lifetime (60 years in this study). Specifically, water usage data is sourced from the IAEA's WAMP software (IEAE, 2018). We apply the following main operational rules to the simulators for both the NPP without reserve and with reserve:

- Water flow limit check: the NPP shuts down if the Po River flow drops below the low-flow limit.
- Concurrent checks: simultaneously verify that water withdrawal does not exceed the maximum percentage of river flow and that the discharged water temperature does not exceed 35 °C.
- Reserve level management: the reserve has three fixed levels—low, medium, and high. The NPP operates at full capacity above the high level, at 75 % capacity between the medium and high levels, at 50 % capacity between the low and medium levels, and shuts down below the low level.
- Water flow limit check: reserve intake is prohibited if the river flow drops below the low-flow limit. However, the NPP can still produce power if reserved water is available.
- Reserve intake calculation: determine the allowable water intake based on the regulatory limit and pump capacity.
- Power production dependency: power production directly depends on the reserve level, with river flow utilized solely for reserve water intake.
- Both scenarios also incorporate a three-day buffer to prevent frequent shutdowns and startups caused by fluctuations in river flow near the lower regulatory intake limit.

Fig. 5 and Fig. 6 present the simulation logical flow for the NPP case without the reserve and with the reserve, respectively.

3.3.2. NPV_{CO2e} computation

After executing all simulations, several steps are undertaken to calculate the NPV_{CO2e}. The dataset comprises over 1,000 simulations, each containing daily data from 2020 to 2080, including:

- Average daily river flow, river water temperature, air temperature, and relative humidity.
- Without reserve: daily energy produced [MWh], Water consumption [m^3].
- With reserve: reserve intake [m^3], water consumption [m^3], reserve level [m^3], daily energy produced [MWh].

Initially, emissions were only considered for calculating the option price, exercise price, and operational costs. Now, CI data is used to compute the actualized emissions saved, expressed in tons of CO_2e/MW_h:

$$S_e(t) = E_p(t) \times (CI_c(t) - CI_n) \tag{7}$$

where:

- $S_e(t)$ [tonCO_2e] is the value of saved emissions,
- $E_p(t)$ [MW_h] is the energy the NPP produces in year t,
- $CI_c(t)$ [ton CO_2e/MW_h] is the forecasted carbon intensity of the country for year t,
- CI_n is the carbon intensity of nuclear power, assumed to be 0.005 tonCO_2e/MW_h (UNECE, 2022), and
- t_0 is the current year.

To evaluate the option to invest in the reserve, the difference in actualized emissions between scenarios with and without the reserve is calculated:

$$\Delta S_e(t) = S_e(t)_{with\_reserve} - S_e(t)_{without\_reserve} \tag{8}$$

Finally, the NPV_{CO2e} is computed by accounting for the Weighted Average Cost of CO_2e (WACCO_2e) and depending on the year t_i of the investment:

$$NPV_{CO2e} = \frac{\Delta S_e(t) - P_e(t) - O_e(t)}{(1 + WACCO_2e)^{t-t_i}} - P_O \tag{9}$$

where:

- P_o is the option price,
- $P_e(t)$ is the exercise price (see Eq. (3)), and
- $O_e(t)$ is the operating emissions (see Eq. (6)).

Eq. (9) implies that the year of investment t_i can differ from the current year t_0. It is prudent to assess the investment as if it were made both today and, in the future, evaluating all possible investment windows. Additionally, considering the asymmetry between the NPP's expected lifetime (60 years) and the reserve's expected lifetime (20 years), the model assumes that the option exercise price $P_e(t)$ is exercised every 20 years from the investment date until the end of the NPP's lifetime.

4. Results

This section presents the ROA results evaluated for the three CI scenarios in Fig. 3. This section includes three subsections. In the first subsection the overall NPV_{CO2e} distributions are examined, providing insight into the potential outcomes under different conditions (Section 4.1). The second subsection delves into the sensitivity analysis results, which assess how changes in key parameters affect the NPV_{CO2e} distributions (Section 4.2). The third subsection plots the results of the option to wait for one trigger threshold (Section 4.3). For consistency, purple always refers to the worst case, green to the base case, and yellow to the best case.

4.1. NPV_{CO2e} analysis

Fig. 7 presents the distributions of NPV_{CO2e} under the best-, base-, and worst-case scenarios. The proportion of simulations yielding a positive NPV_{CO2e} is 99.17 % for the best case, 84.39 % for the base case, and 22.84 % for the worst case. Fig. 8 reports the corresponding CO_2e costs. Most of these costs are driven by the additional pump, which is particularly high due to its continuous operation at the national CI level (see Eq. (6)).

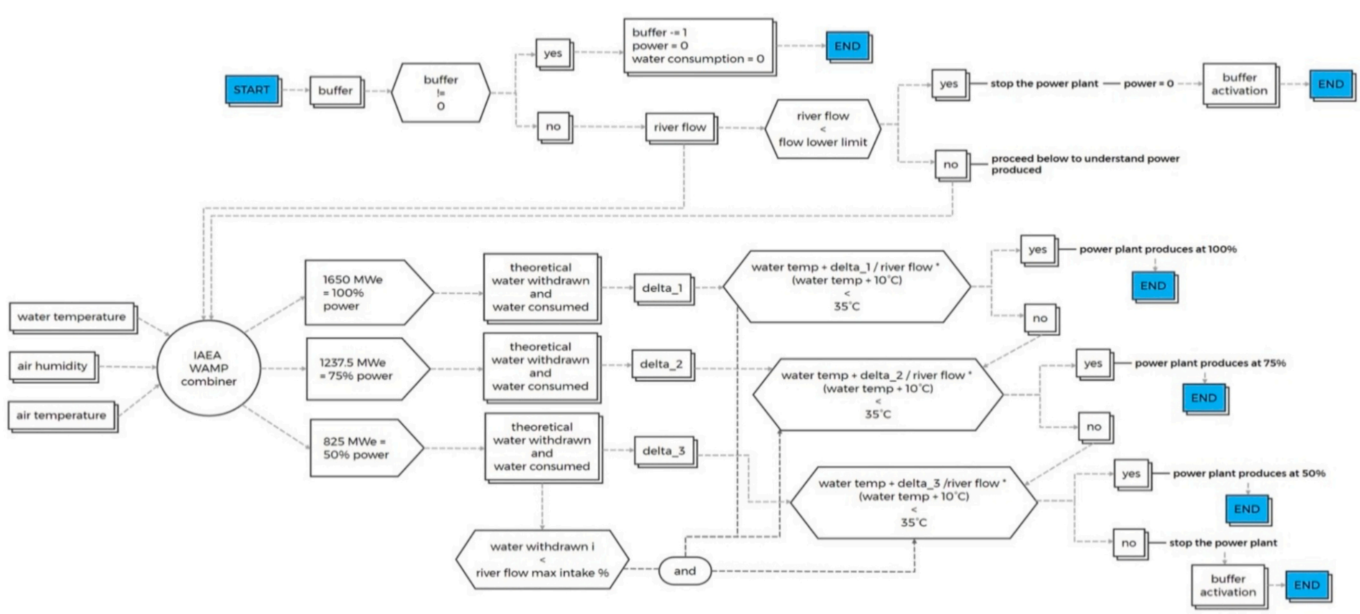

Fig. 5. NPP without reserve simulation logic.

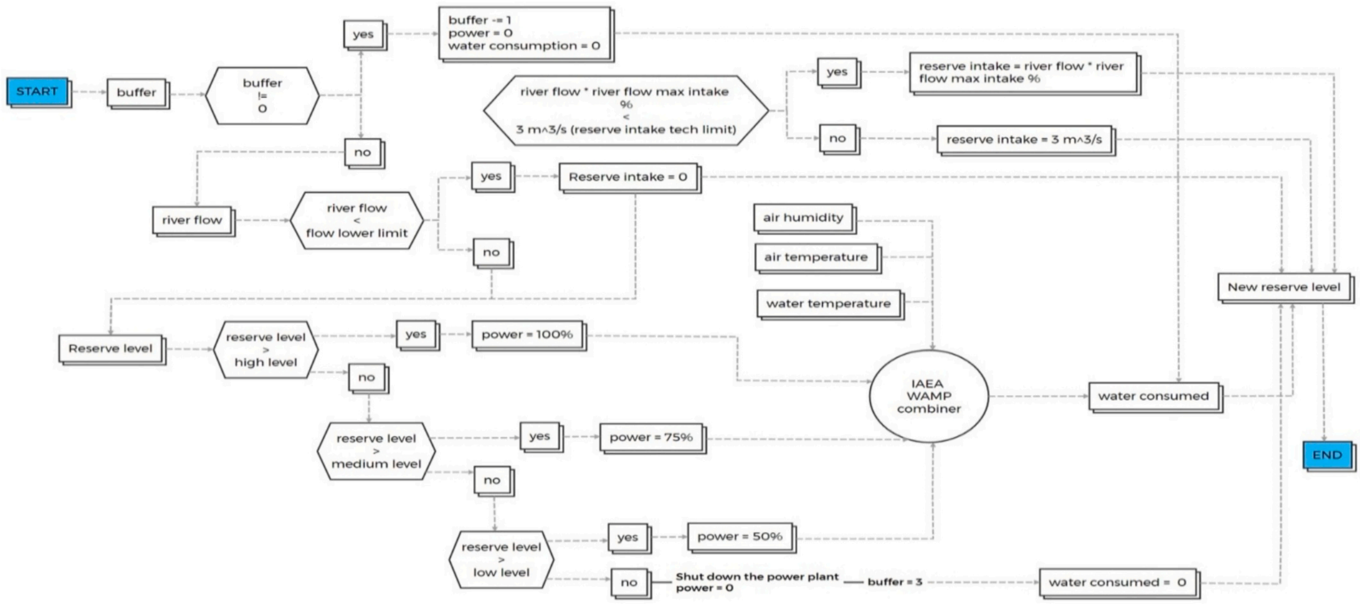

Fig. 6. NPP with reserve simulation logic.

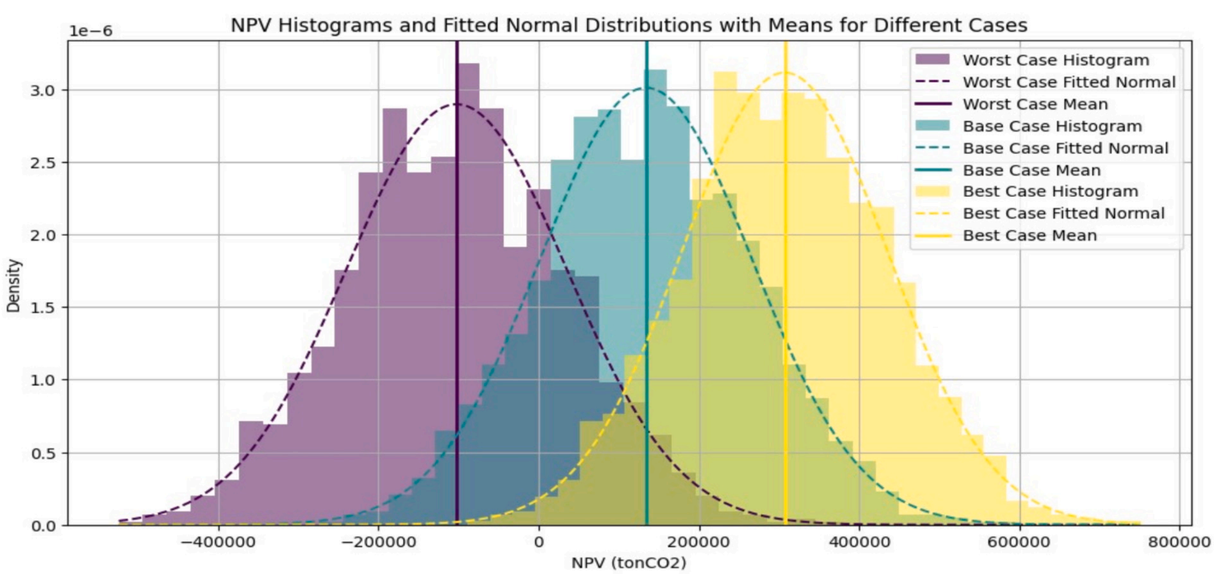

Fig. 7. NPV_{CO2e} distributions of worst (purple), base (green), and best (yellow) scenarios. (For interpretation of the references to colour in this figure legend, the reader is referred to the web version of this article.)

4.2. Sensitivity analysis

The sensitivity analysis shows how parameters changes affect the mean and standard deviation of the NPV_{CO2e} distributions. The NPV_{CO2e} is derived from the difference in emissions saved by the NPP with and without the reserve. Therefore, to explain the NPV_{CO2e}, it is essential to consider both scenarios, NPP operation with and without the reserve. This explanation is provided for each sensitivity parameter that impacts the NPP's load factors. Table 2 presents the parameters used in the sensitivity analysis.

The sensitivity analysis in this study is designed to explore the impact of key parameters on the NPP performance and CO_2 reduction outcomes under varying operational and environmental conditions. The low-flow threshold is set at 270 m^3/s for the base case, corresponding to the "severe drought" category according to the SDI, with a probability of approximately 4.4 %. This threshold varies between 200 and 340 m^3/s to capture different interpretations of drought severity and regulatory risk tolerance. This ensures that the model reflects realistic operational limits during extreme low-flow events while maintaining ecological protection. This range spans extremely conservative withdrawals to scenarios accommodating peak NPP demand, allowing exploration of environmental and policy trade-offs. The Palo Verde NPP serves as a reference for reserve size and depth. The base-case reserve is 0.9 million m^3, scaled to match the full-power cooling requirements of the 1,000 MWe NPP under study. The option price for enabling works is 25,000 tCO_2e, reflecting embodied carbon in reinforced concrete and steel for civil infrastructure. HDPE liner emissions are explored from 0 to 16 tCO_2e/ton, with a base case of 8 tCO_2e/ton, accounting for both resin production and downstream processing uncertainties. Sensitivity is displayed in Fig. 9.

From the sensitivity analysis emerges that:

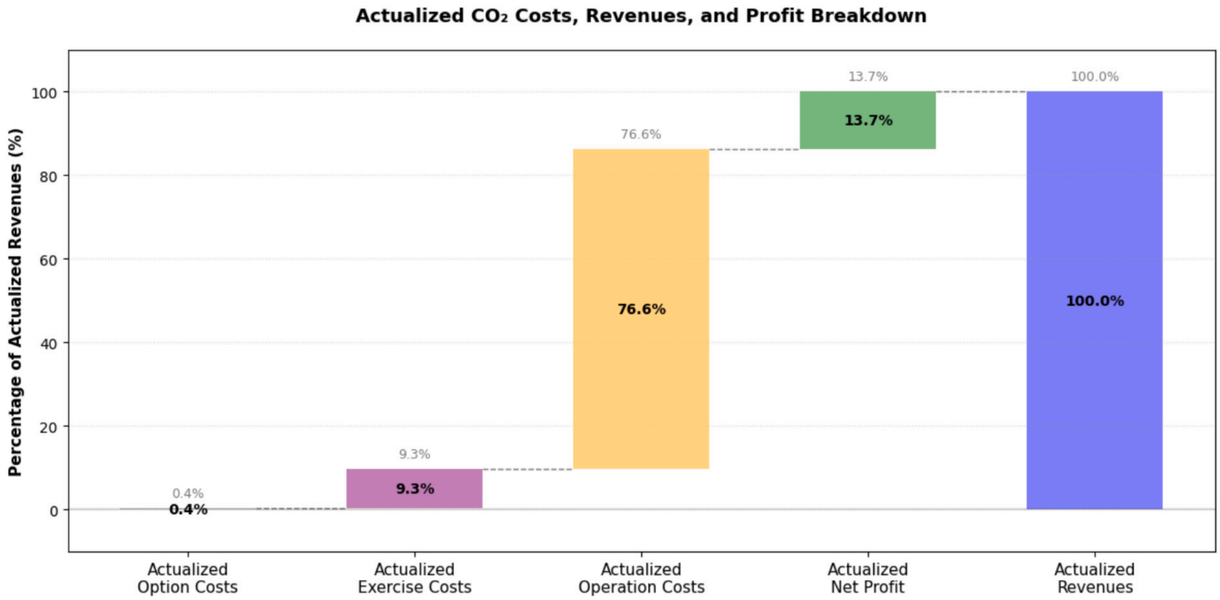

Fig. 8. Actualized costs, revenues and profit breakdown. Analysis with WACCO_2e = 4 % and inflation rate = 1.5 %.

Table 2
Parameters subject to sensitivity analysis.

Type	Parameter	Sensitivity	Units of measurement
Regulation	Low-Flow limit	200–340	m^3/s
Regulation	Flow % limit	0.001–1	%
Optimization	Reserve size	4–100	Days of Full Power Operation (DFPO)
Prices	Reserve depth	3–15	m
Prices	Option Price	0–50,000	tonCO_2e
Prices	HDPE cost	0–16	tonCO_2e/ton(material)

- The NPP without a reserve must shut down when the regulatory limit is reached.
- The NPP with a reserve can continue to operate using the stored water.

The higher the low-flow regulatory limit, the greater the NPV_{CO2e} of the reserve. This is because a higher limit would increase the frequency of reserve usage. Conversely, if the limit is set too low, the costs of maintaining the reserve would outweigh the additional energy produced. Specifically, the threshold between average profitability and unprofitability is 263 m^3/s, corresponding to a river flow probability of 4.1 % (SDI = −2.1). This indicates that if regulators set the lower limit above this threshold, investing in the water reservoir would, on average, be profitable; otherwise, it would not. The second parameter is the maximum percentage of daily river flow that the NPP can intake. Sensitivity analysis is shown in Fig. 10. This parameter prevents the reserve from withdrawing too much water in a single day, which could result in environmental issues.

The analyzed values range between 0 and 1 %, and if the constraint is met:

- The NPP without reserve should decrease power when this value is reached.

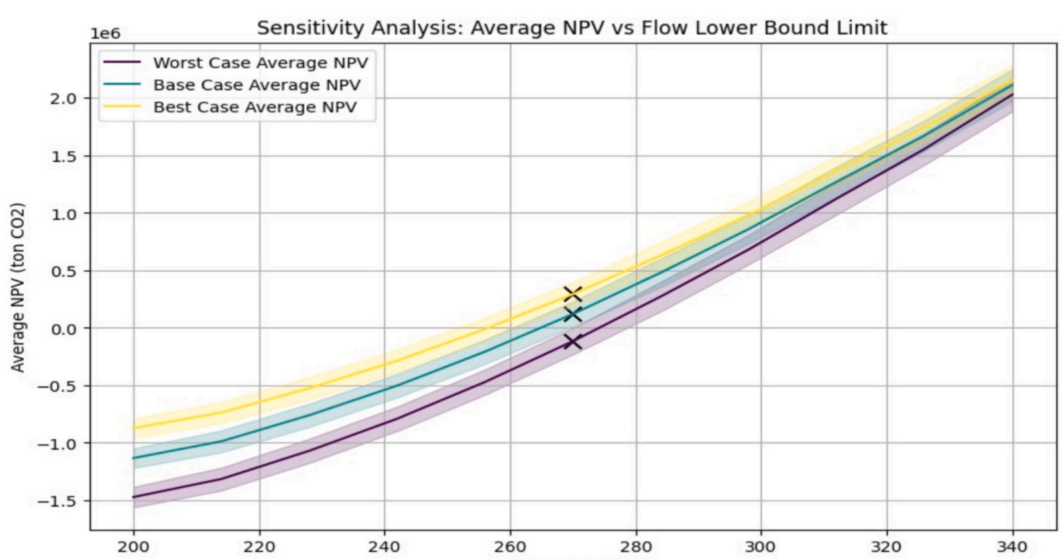

Fig. 9. Sensitivity analysis on the low-flow boundary regulatory limit.

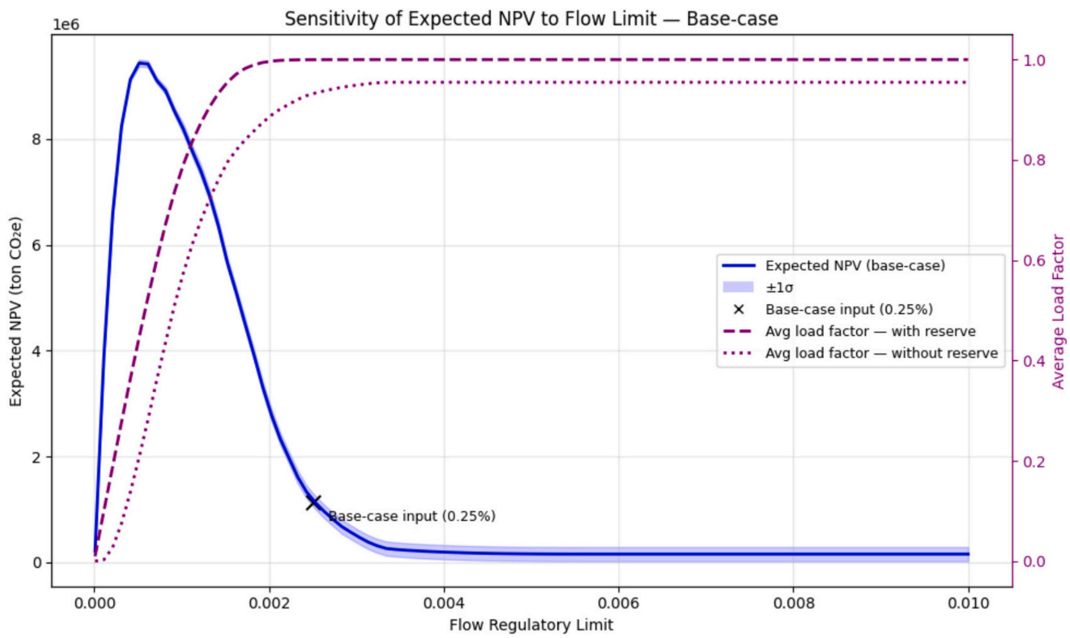

Fig. 10. Sensitivity of expected NPVCO2e to the flow regulatory limit (base-case CI scenario). **Legend:** Blue line shows the expected NPV_{CO2e}; the shaded band indicates ±1 standard deviation. The "×" marks the base-case input (0.25 % = 0.0025). Purple curves (right y-axis) report the average simulated load factors for the configurations with (dashed) and without (dotted) the reserve. (For interpretation of the references to colour in this figure legend, the reader is referred to the web version of this article.)

- The NPP with the reserve would intake the amount of water at the limit point (to maximize the intake).

Low percentages significantly favour the reserve. At the same time, the second result relies on the two purple lines, which indicate the NPP's average simulated load factors, and pinpoint that the regulator should consider when deciding the tailored power NPP limit. If the limit is set higher than 0.3 %, both the NPPs would be at their maximum load factor possible, and the reserve would be less reasonable, still being profitable.

4.2.1. Optimal reserve size

This sensitivity analysis allows decision-makers to optimize the reserve size. Fig. 11 shows that the optimal reserve sizes in all the scenarios are 15 days of equivalent full power capacity (900,000 m^3 of water – see Eq. (1)). Between 10 and 19 days, the average NPV_{CO2e} in all the scenarios is positive, while under 8 days, there is almost certainty that CO_2e will be unprofitable. Decreasing the reserve excessively is not beneficial as the extra reserve capacity would not cover operational costs while increasing the reserve size excessively increases the exercise price, driving the NPV_{CO2e}. The option price minimally impacts the NPV_{CO2e} of the investment (Fig. 12). Instead, the plot of Eq. (3) (Fig. 13) shows the linear dependency of the exercise price on the HDPE cost and the inverse quadratic dependency on the reserve depth.

4.3. Option to wait

The reservoir can be built years after the NPP has been constructed, so that it is not necessarily parallel to the NPP construction. So, the decision maker can build the NPP and wait to see if the reservoir is necessary. In ROA language, this is an option to wait. To assess the value

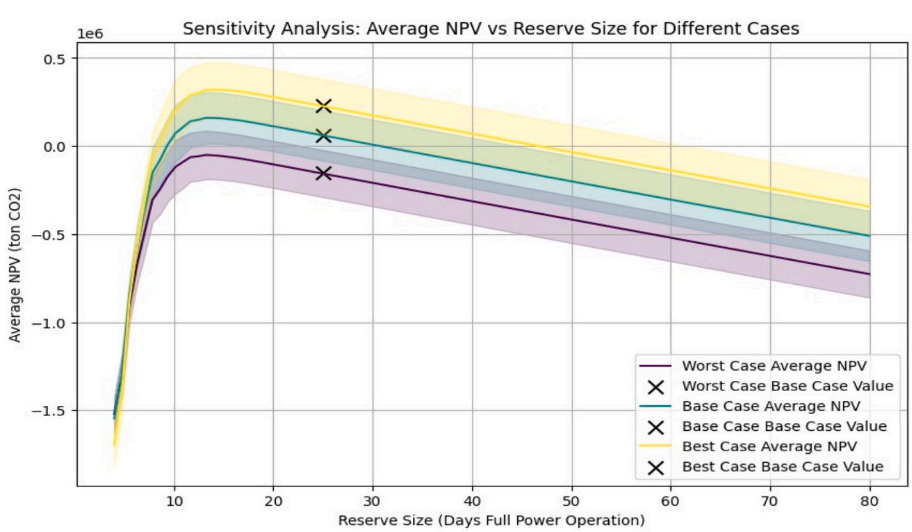

Fig. 11. Sensitivity analysis on reserve size.

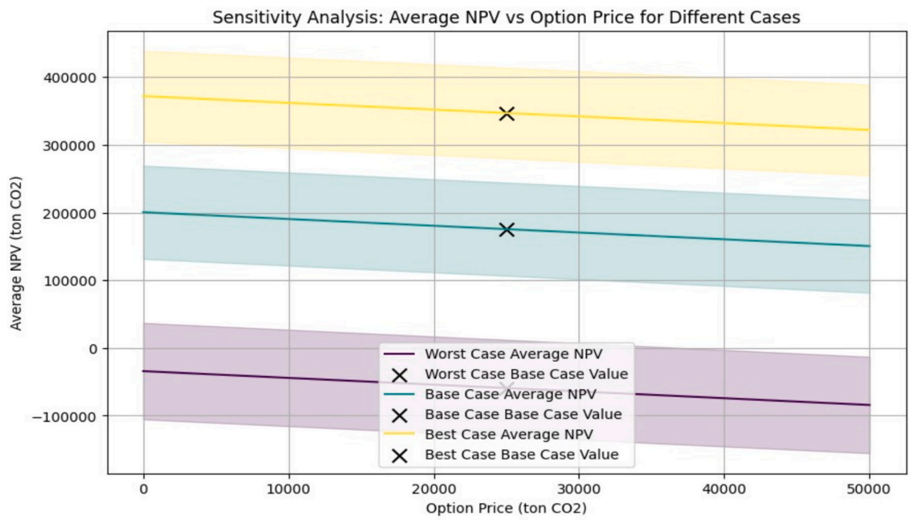

Fig. 12. Sensitivity analysis on the option price.

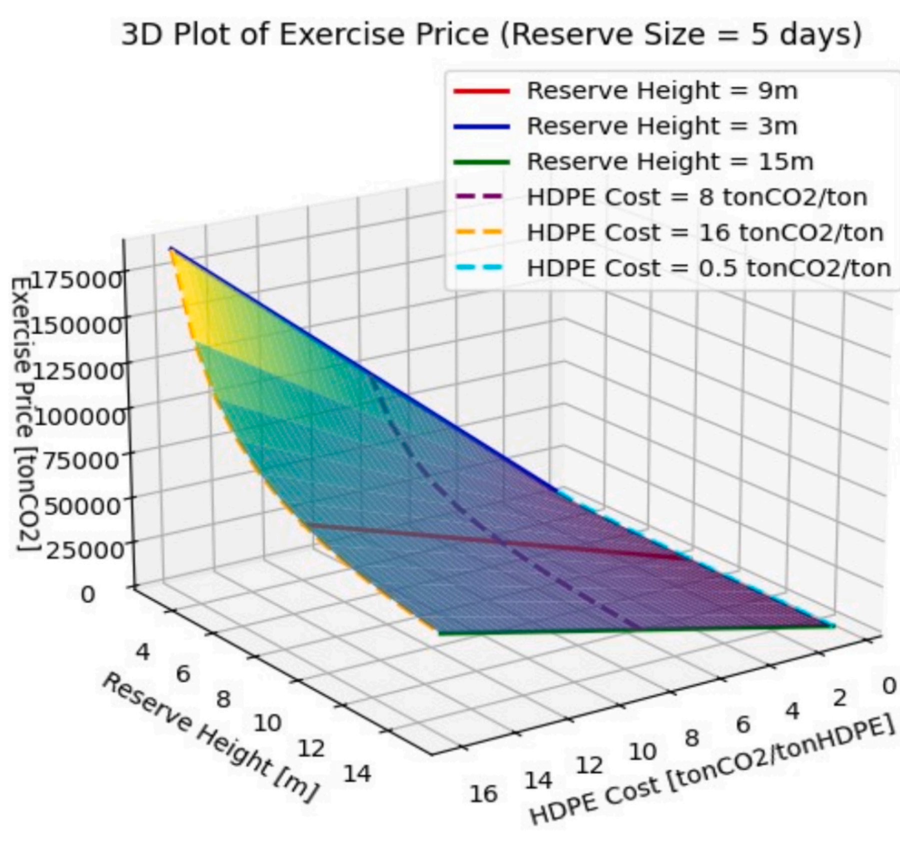

Fig. 13. Option Exercise Price depending on the Reserve Height [m] and HDPE unitary emissions [tonCO_2e/tonHDPE].

of this option, we performed a sensitivity analysis that reflects the same dependencies with respect to the sensitivity parameters (Fig. 14 and Fig. 15). Indeed, HDPE cost and reserve depth do not affect the NPP's load factors, while they instead influence the NPV_{CO2e} by altering the overall cost structure, either increasing or decreasing it.

We derived the option to wait by applying the threshold analysis method (Locatelli et al., 2020) to our model. We analyse a single threshold, which we define as the moving average of river flow over three years. The model simulates exercising the option at different values of this moving average, ranging from 650 to 900 m^3/s, and evaluates the corresponding average NPV_{CO2e} and their standard deviations (Fig. 16). The figure compares the expected NPV_{CO2e} if investing immediately versus waiting for a 3-year moving-average river-flow trigger. The baseline scenario assumes a base-case CI trajectory, defined as Italy's historical average year-on-year reduction in grid CI, with best- and worst-case scenarios constructed as $\pm$0.5 % around this average. Starting from the orange vertical line, the analysis returns that, on average, the time now is the best moment to invest. Moreover, investing using the moving average as a threshold results in lower NPV_{CO2e} than investing directly today. This is due to the threshold of waiting at least 3 years for the moving average.

A cost-revenues-time analysis is drafted to understand better the

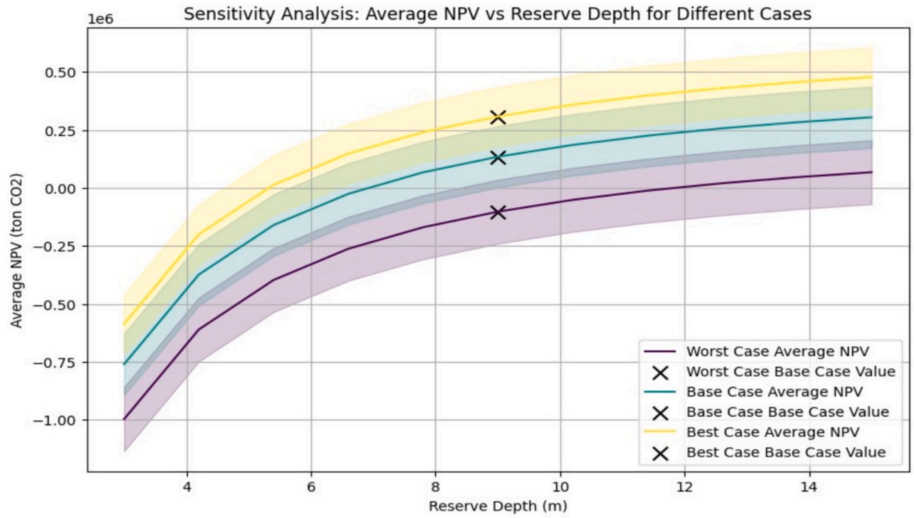

Fig. 14. Sensitivity analysis on the reserve depth.

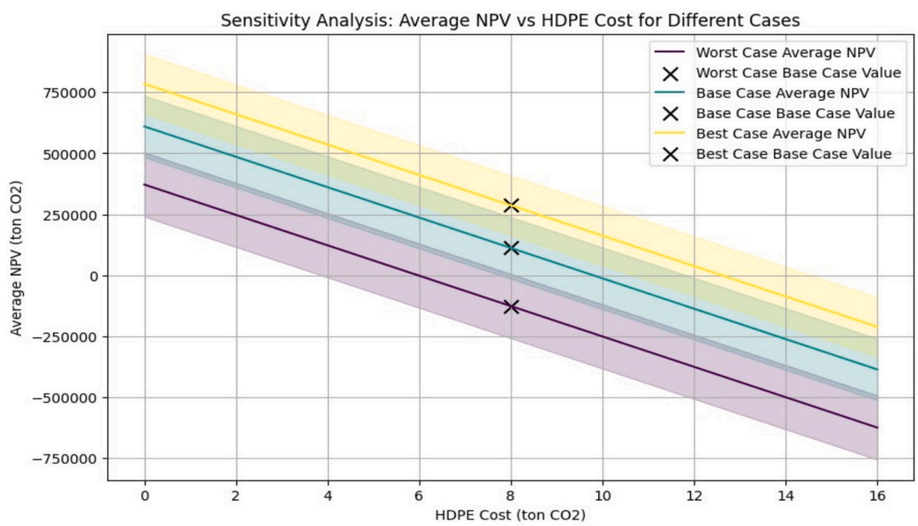

Fig. 15. Sensitivity analysis of the HDPE cost.

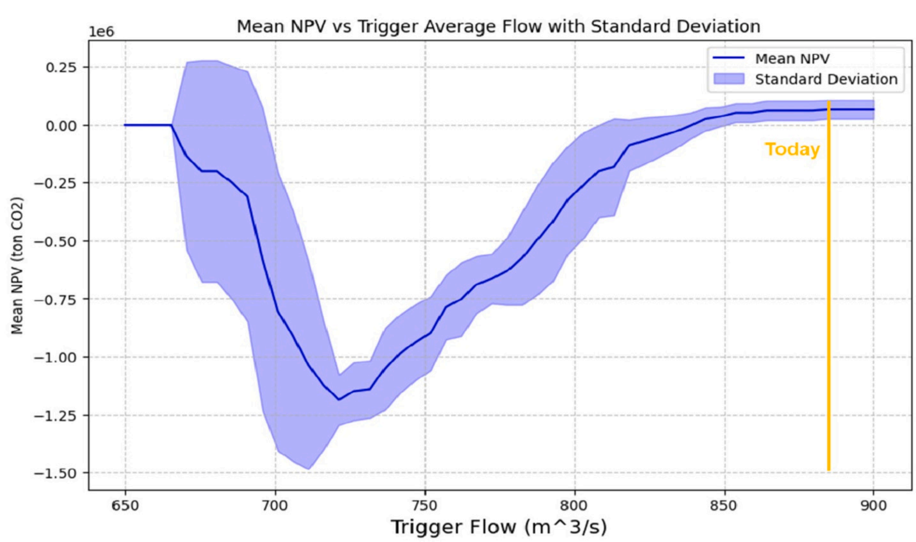

Fig. 16. Option to wait – river flow three-year moving average as trigger threshold.

option to wait, showing how the CI and operation costs drive down CO_2e profits. Fig. 17 shows the average revenues and costs related to the year without discount parameters to thoroughly display the short- and long-term trends.

This analysis shows that, on average, the base case is expected to deliver diminishing returns over time due to the declining trend in CI (Fig. 3). Although the NPP achieves higher emission savings, the CI decreases too quickly to support sustained investment over multiple years. In contrast, when considering average cumulative emissions, the value of the project is better preserved, as it captures the long-term benefits of avoided emissions rather than being penalized by the yearly decline in marginal CI.

Fig. 18 presents the results of the cumulative emissions revenue (saved CO_2e) and cost analysis. The plot shows that the highest NPV_{CO2e} is reached in 2039, indicating that, on average, not reinvesting in the water reserve yields higher returns than proceeding with a second investment. Furthermore, the three-year moving average of river flow never drops below 670 m^3/s; as a result, the model does not simulate investment scenarios below this threshold. This leads to a slightly negative NPV_{CO2e} due to the upfront cost associated with holding the option.

When decision-makers consider delaying investment until the moving average river flow reaches 670–690 m^3/s, the standard deviation of the NPV_{CO2e} increases significantly. This indicates a broader range of potential outcomes: while the expected value remains low, a non-negligible possibility exists, albeit with low probability, of realizing particularly high NPV_{CO2e}. This reflects a classic risk–return trade-off, where the opportunity to capture favorable but unlikely conditions is counterbalanced by increased uncertainty and a greater likelihood of suboptimal outcomes. Therefore, postponing the investment introduces a higher degree of unpredictability, which decision-makers must carefully weigh against the potential for exceptional gains.

5. Conclusions and future developments

In this paper, we developed a CO_2-based real options framework that integrates an enhanced LCA with MCS–based ROA to evaluate how external events (demonstrated here with drought) alter the NPP life-cycle CO_2e performance, measured by evaluating the NPV_{CO2e}. The model explicitly translates investment choices (e.g., building a backup reservoir) into embodied and operational CO_2e costs and avoided CO_2e savings. We applied the model to a pseudo-real 1,000 MWe PWR on the Po River. This study contributes to the literature on nuclear power planning and low-carbon infrastructure by proposing an innovative model that integrates enhanced LCA with ROA under uncertainty, using CO_2e emissions as the primary evaluation metric. The model developed in this study reveals a critical dynamic (IAEA, 2023; IEA, 2025): while droughts caused by drier rivers diminish the output of NPPs, the lower CI of the grid may reduce the effectiveness of investing in reservoirs solely for CO_2e savings. The model provides a detailed analysis of this nuanced scenario tailored to the specific location of the NPP under study. It incorporates several key factors, including probabilistic models of uncertain drought conditions, projections of future CI, regulatory limits on water use, and the associated emissions costs. This comprehensive approach offers a holistic perspective on the trade-offs involved in reservoir investments in nuclear power in a low-carbon future. Immediate investments in water reservoirs can provide significant environmental benefits by reducing emissions, particularly in the context of climate-related drought mitigation. However, the model shows that future investments in water reservoirs might yield diminishing returns as the grid continues decarbonizing through renewable energy integration. Therefore, timing plays a critical role: investments made during the NPP commissioning phase offer the highest NPV_{CO2e} and environmental returns compared to those delayed. The model suggests that the maximum NPV_{CO2e} is achieved by exercising the option to invest in the water reservoir during the NPP commissioning phase and not reinvesting after the initial 20-year reservoir lifetime. This implies that after 20 years, when the reservoir needs relining or reconstruction, it may no longer be environmentally viable, given the advancements in grid decarbonization.

In summary, the key finding is therefore that reservoir investments can be CO_2e-beneficial under a wide range of plausible hydrological and regulatory conditions: positive NPV_{CO2e} occurs in the majority of best- and base-case scenarios, while results become marginal in pessimistic CI trajectories or stringent regulatory envelopes. Key sensitivities include the regulatory low-flow threshold and reserve size (optimal ≈15 days of full-power equivalent in our case). The analysis reveals an important timing effect: exercising the option to build a reservoir at NPP commissioning yields larger CO_2e returns on average than deferring investment, because progressive grid decarbonization reduces the marginal avoided emissions over time. However, an option to wait can still be valuable when uncertainty around hydrology or policy is large.

The theoretical implications are mainly three.

First, the model enhances LCA by incorporating the impact of external events, such as droughts, on the actual operational performance of NPPs, thus addressing the standard limitation of idealized, uninterrupted project life-cycles in traditional environmental assessments (Bauer et al., 2015; Nock and Baker, 2019). This aligns with recent calls in the literature for dynamic, risk-informed appraisal methods that move beyond static LCA assumptions and recognize the systemic vulnerability

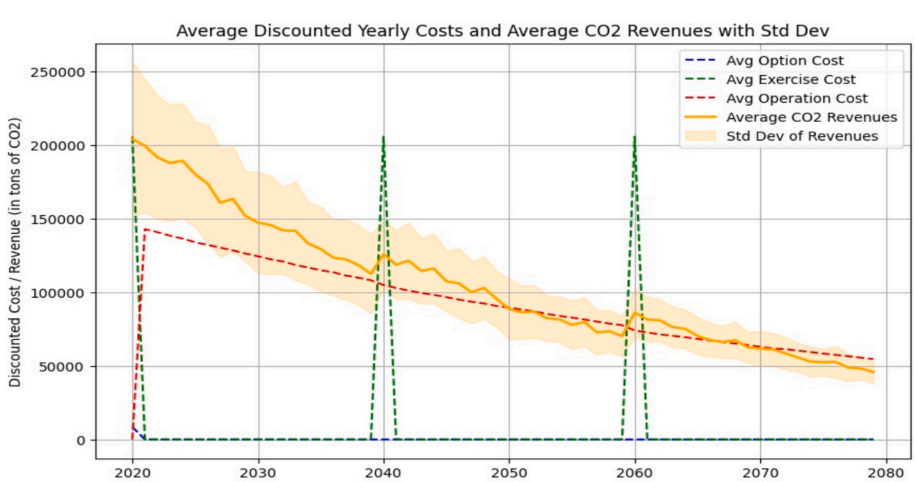

Fig. 17. CO2eq revenues and costs over time.

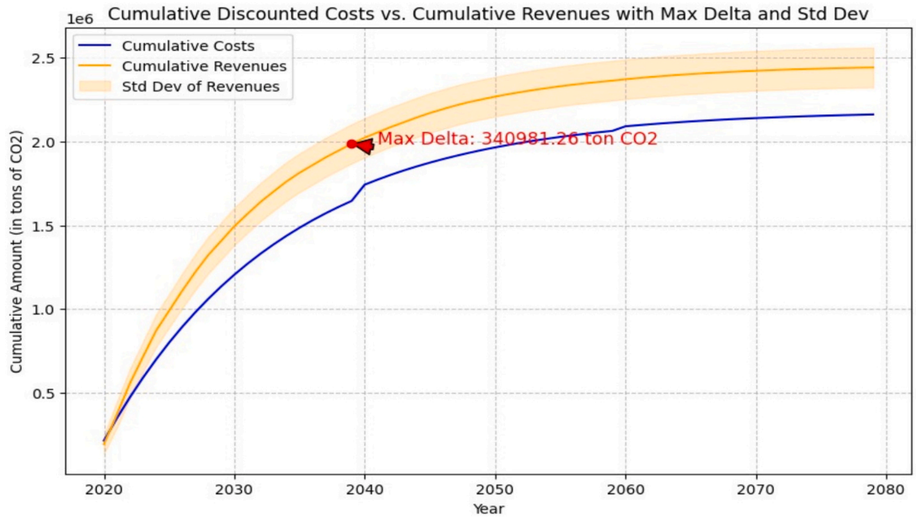

Fig. 18. Cumulative emissions revenues (saved CO_2e) and costs.

of large-scale energy infrastructures (Pucciarelli et al., 2024).

Second, it introduces a novel ROA formulation that evaluates investment flexibility based not on financial returns, but on environmental performance, specifically CO_2e emissions. By reframing ROA around carbon performance rather than monetary value, the model expands the applicability of financial tools to domains where environmental objectives are primary, thus bridging the gap between environmental assessment and investment planning under uncertainty (Locatelli et al., 2015; Cardin et al., 2020). This perspective is particularly relevant for technologies like NPPs, where carbon returns are realized over extended periods and are highly sensitive to disruptive events (Kiriyama and Suzuki, 2004; Arasteh, 2024).

Third, it embeds uncertainty by simulating multiple CO_2 emission scenarios, offering decision-makers a more realistic appraisal of long-term carbon impacts of external events (e.g., droughts). Drought is a significant risk affecting NPPs (Raso et al., 2019), jeopardizing their performance as water scarcity worsens due to climate change (Rossi et al., 2023). However, the existing literature primarily lacks proactive drought mitigation strategies and concentrates on traditional water management programs and efficiency improvements (IEAE, 2018). This focus has created a notable gap in developing models that evaluate investments to mitigate drought risks in NPP operations (Middleton et al., 2021). Addressing this gap, this study proposes and evaluates a flexible option (i.e., constructing a water reservoir), and assesses uncertainties related to environmental variables, such as drought scenarios and future CI.

The empirical implications are practical insights for decision-makers planning and regulating low-carbon energy infrastructure. The model is a decision support tool that bridges technical planning with environmental policy, enabling a more integrated and adaptive approach to infrastructure investment under climate risk. The proposed approach allows decision-makers to postpone investment until more accurate forecasts of key variables, such as national CI and hydrological conditions, become available. This option to wait adds strategic flexibility and reduces exposure to uncertainty, particularly in contexts where policy or climate trajectories are volatile.

The model provides a framework for public authorities and policymakers to design and evaluate incentive schemes based on environmental rather than purely financial performance. Simulating multiple future scenarios makes it possible to assess how targeted subsidies, carbon pricing, or capacity payments could improve the environmental return on investment (measured in CO_2e savings) while supporting national energy mix goals. This is especially relevant in countries seeking to integrate nuclear energy into their decarbonization strategy under growing climatic and operational uncertainties. Moreover, using probabilistic simulation tools and enhanced LCA can help regulatory bodies adopt more robust and risk-informed planning procedures, ensuring that investments deliver expected climate benefits even under adverse conditions.

Concerning limitations, despite its embedded generality, the present framework remains an exploratory implementation. Modelling assumptions, particularly in representing hydrological variability, the temporal evolution of grid CI, and the treatment of embodied CO_2e in enabling infrastructure are simplified to preserve analytical transparency. These choices enhance interpretability but inevitably narrow quantitative precision. Moreover, correlations among environmental, operational, and policy uncertainties are only partially captured, which may understate compound or cascading effects during extreme events. Finally, the application to a pseudo-real case study limits direct extrapolation to specific sites or reactor technologies; the primary contribution lies in demonstrating methodological transferability rather than producing site-specific numerical forecasts.

With respect to future direction, this research paves the way for three strands of research.

First, the complexity of the developed model could be increased. Future work could adopt MCS for environmental variables and CI forecasts, thus better capturing the uncertainties in future grid decarbonization. Additionally, introducing correlations between weather variables such as air temperature, water temperature, and relative air humidity would enhance the model's accuracy.

Second, this study could be extended by including a detailed economic analysis alongside the environmental model to provide a more comprehensive assessment for investors. This would offer a dual perspective on the financial and environmental viability of investing in reservoir systems to enhance drought resilience, helping investors make more informed decisions in a rapidly evolving energy landscape.

Third, the proposed model can be further extended to assess other types of risks that may affect the reduction of green CO_2e emissions from the NPP. For instance, seismic risk could be analyzed by evaluating the implementation of advanced isolation systems in the NPP foundations. In this case, the model would help determine whether the additional CO_2e emissions required to build such reinforced foundations are offset by the extra electricity produced in the event of an earthquake, when the NPP remains operational. Similarly, the model could be adapted to account for grid reliability issues or surpluses of renewable electricity production, by considering the installation of electrical (e.g., lithium batteries) or thermal storage systems (e.g., molten salt). The analysis would then assess whether the CO_2e emissions associated with constructing these storage systems are compensated by the increased electricity output during grid instability or renewable oversupply. By adapting the model's parameters and boundary conditions, researchers and decision-makers can use this framework to assess the implications of various external risks on environmental outcomes, ultimately supporting more resilient and informed planning of energy infrastructures.

CRediT authorship contribution statement

Alessandro Paravano: Writing – original draft, Supervision, Methodology, Investigation, Formal analysis, Data curation, Conceptualization. **Giacomo Galeotti:** Writing – original draft, Visualization, Software, Investigation, Formal analysis, Data curation. **Alessandra Neri:** Writing – original draft, Supervision, Data curation, Conceptualization. **Enrico Cagno:** Writing – original draft, Supervision, Investigation, Conceptualization. **Giorgio Locatelli:** Writing – original draft, Visualization, Supervision, Resources, Project administration, Methodology, Funding acquisition, Conceptualization.

Declaration of competing interest

The authors declare the following financial interests/personal relationships which may be considered as potential competing interests: The authors reports that financial support was provided by Italian Ministry of University and Research. Yet, they declare that they have no known competing financial interests or personal relationships that could have appeared to influence the work reported in this paper.

Acknowledgments

This work has been supported by Ministero dell'Università e della Ricerca, PIANO NAZIONALE DI RIPRESA E RESILIENZA (PNRR), Missione 4 "Istruzione e Ricerca" – Componente C2 Investimento 1.1, "Fondo per il Programma Nazionale di Ricerca e Progetti di Rilevante Interesse Nazionale (PRIN)" Grant number 2022J534JS.

Appendix A: Streamflow Drought Index (SDI) assumptions

SDI measures hydrological drought based on river flow, whereas the SPI measures meteorological drought based on precipitation. The SDI is defined as (Nalbantis and Tsakiris, 2009):

$$SDI_{i,k} = \frac{y_{i,k} - y_k}{s_{y,k}}$$

where:

- $i = 1,2, \ldots$ represents the year;
- $k = 1,2,3,4$ denotes the season;
- $yi,k = \ln(Vi,k)$ is the natural logarithms of cumulative streamflow $V_{i,k}$;
- The mean y_k and standard deviation $s_{y,k}$ are estimated over a long period of time.

The definition of states of hydrological drought using SDI is described in Table A1.

Table A1
SDI states.

State	Description	Criterion	Probability (%)
0	Non-drought	$SDI \geq 0.0$	50.0
1	Mild drought	$-1.0 \leq SDI < 0.0$	34.1
2	Moderate drought	$-1.5 \leq SDI < -1.0$	9.2
3	Severe drought	$-2.0 \leq SDI < -1.5$	4.4
4	Extreme drought	$SDI < -2.0$	2.3

Data availability

Data will be made available on request.

References

Adamov, E., et al., 2025. Nuclear power engineering with fast neutron reactors and closed nuclear fuel cycle – solution of climate problems and more. Nucl. Eng. Des. 433, 113803. Available at: https://doi.org/10.1016/j.nucengdes.2024.113803.

Almeida, M., et al., 2021. The probability distribution of daily streamflow in perennial rivers of Angola. J. Hydrol. 603 (126869).

Aminsharei, M.H., Nikbin, I.M., Sani, H.P., 2024. Radiation shielding properties of heavy-weight concrete and heavy-weight geopolymer concrete incorporating nano-ZnS. Nucl. Eng. Des. 424, 113240. Available at: https://doi.org/10.1016/j.nucengdes.2024.113240.

Arasteh, A., 2024. Application of real options valuation in nuclear energy systems. Int. J. Res. Ind. Eng. 13 (3), 274–305. Available at: 10.22105/riej.2024.443054.1421.

ARPAE (2024) Dati e osservazioni, Arpae Emilia-Romagna. Available at: https://www.arpae.it/it/temi-ambientali/meteo/dati-e-osservazioni (Accessed: May 30, 2025).

ARPAE-SIMC (Regional Agency for Prevention, Environment and Energy of Emilia-Romagna – Hydro-Meteo-Climate Service), 2024. Dext3r: Web application for the extraction of hydro-meteorological data. Available at: https://simc.arpae.it/dext3r/ (Accessed: November 2024).

Bauer, C., et al., 2015. The environmental performance of current and future passenger vehicles: life cycle assessment based on a novel scenario analysis framework. Appl. Energy 157, 871–883. Available at: https://doi.org/10.1016/j.apenergy.2015.01.019.

Box, G.E.P., et al., 2015. Time Series Analysis: Forecasting and Control, 5th ed. Wiley. Available at: https://www.wiley.com/en-us/Time+Series+Analysis%3A+Forecasting+and+Control%2C+5th+Edition-p-9781118675021. (Accessed 12 June 2025).

Bureau of Energy Efficiency, 2004. Cooling tower. In: India. pp. 135–151. Available at: https://beeindia.gov.in/sites/default/files/3Ch7.pdf.

Cardin, M.-A., Zhang, S., Nuttall, W.J., 2017. Strategic real option and flexibility analysis for nuclear power plants considering uncertainty in electricity demand and public acceptance. Energy Econ. 64 (C), 226–237.

Cardin, M.-A., Mijic, A., Whyte, J., 2020. Flexibility and real options in engineering systems design. In: Maier, A., Oehmen, J., Vermaas, P.E. (Eds.), Handbook of Engineering Systems Design. Springer International Publishing, Cham, pp. 1–29. Available at: https://doi.org/10.1007/978-3-030-46054-9_35-1.

Crellin, F. (2024) "Hot river water curbs output at French nuclear plant," Reuters, 2 August. Available at: https://www.reuters.com/business/energy/hot-river-water-curbs-output-french-nuclear-plant-2024-08-02/ (Accessed: October 28, 2025).

Durighetto, N., et al., 2022. Probabilistic description of streamflow and active length regimes in Rivers. Water Resour. Res. 58 (4).

EDO, 2025. Standardized Precipitation Index. European Union: European Drought Observatory, pp. 1–6. Available at: https://drought.emergency.copernicus.eu/data/factsheets/factsheet_spi.pdf. (Accessed 30 May 2025).

ERG Franklin Associates, A.D., 2020. Cradle-Togate Life Cycle Analysis of Highdensity Polyethylene (HDPE) Resin. Final Report. American Chemical Council, USA.

Faizan, M., et al., 2024. Thermal energy storage integration with nuclear power: a critical review. J. Energy Storage 96, 112577.

Frapin, M., et al., 2022. Modelling long-term and short-term temporal variation and uncertainty of electricity production in the life cycle assessment of buildings. Appl. Energy 307, 118141. Available at: https://doi.org/10.1016/j.apenergy.2021.118141.

Declaration to Triple Nuclear Energy, 2023. Baku. Available at: https://world-nuclear.org/images/articles/Declaration-to-Triple-Nuclear-Energy-_-COP28-_-28-November-2023-FINAL.pdf (Accessed: May 29, 2025).

Giliberto, J. (2022) "La grande magra del Po ferma le centrali termoelettriche," Il Sole 24 ORE, 20 June. Available at: https://stream24.ilsole24ore.com/embed/AELmR9gB (Accessed: May 30, 2025).

Global Carbon Budget et al. (2025). Carbon intensity of energy production." Global Carbon Project; U.S. Energy Information Administration; Energy Institute. Available at: https://archive.ourworldindata.org/20250909-093708/grapher/co2-per-unit-energy.html (Accessed: September 9, 2025).

Gupta, V.K., Waymire, E., 1990. Multiscaling properties of spatial rainfall and river flow distributions. J. Geophys. Res. Atmos. 95 (D3), 1999–2009.

Houghtalen, R., Akan, O., Hwang, N., 2016. Fundamentals of Hydraulic Engineering Systems, 5th ed. Pearson College Div. https://www.pearson.com/en-us/subject-catalog/p/fundamentals-of-hydraulic-engineering-systems/P200000003144/9780137525768?srsltid=AfmBOor7O_iY4wd6gjgMORfu1BQ6U2R-B3Eqmxwn7V7hvxNrcJTepP5X

Hydro, K., Corporation, N.P., 2019. APR1000 - Advanced Power Reactor 1000. Technical report. Korea Hydro and Nuclear Power Corporation, Republic of Korea.

IAEA, 2004. Operating Experience with Nuclear Power Stations in Member States in 2003. INTERNATIONAL ATOMIC ENERGY AGENCY (Operating Experience with Nuclear Power Stations in Member States), Vienna. Available at: https://www.iaea.org/publications/7195/operating-experience-with-nuclear-power-stations-in-member-states-in-2003.

IAEA, 2012. Efficient Water Management in Water Cooled Reactors. IAEA, Vienna, p. NP-T-2.6 (IAEA nuclear energy series,.

IAEA, 2018. Efficient Water Management in Water Cooled Reactors. NP-T-2.6. International Atomic Energy Agency, Vienna, p. 131. Available at: https://www-pub.iaea.org/MTCD/Publications/PDF/P1569_web.pdf.

IAEA, 2023. Integrated life cycle risk Management for new Nuclear Power Plants. In: STI/pub/2047. International Atomic Energy Agency, Vienna, Austria, pp. 1–170. Available at: https://www-pub.iaea.org/MTCD/Publications/PDF/P2047_web.pdf.

IAEA (2022) *Climate Change and Nuclear Power 2022.* Technical report,. Vienna, Austria: IAEA. Available at: https://www.iaea.org/sites/default/files/iaea-ccnp2022-body-web.pdf.

IEA, 2025. The Path to a New Era for Nuclear Energy. France, International Energy Agency, pp. 1–102. Available at: https://www.iea.org/reports/the-path-to-a-new-era-for-nuclear-energy. (Accessed 29 May 2025).

IEAE, 2018. Efficient Water Management in Nuclear Power Plants. IAEA, Publisher.

IPCC (2021) "IPCC, 2021: Summary for Policymakers. In: Climate Change 2021: The Physical Science Basis. Contribution of Working Group I to the Sixth Assessment Report of the Intergovernmental Panel on Climate Change." Available at: https://doi.org/10.1017/9781009157896.001 (Accessed: November 4, 2024).

IPCC, WMO, and UNEP, 2022. Climate Change 2022. Mitigation of Climate Change.

Italian Government (2006). d.lgs. n. 152/2006, 152/2006. Available at: https://www.bosettiegatti.eu/info/norme/statali/2006_0152.htm (Accessed: May 30, 2025).

Jain, S., Roelofs, F., Oosterlee, C.W., 2013. Valuing modular nuclear power plants in finite time decision horizon. Energy Econ. 36 (C), 625–636.

Jeon, H., 2019. Licensing and information disclosure under asymmetric information. Eur. J. Oper. Res. 276 (1), 314–330. Available at: https://doi.org/10.1016/j.ejor.2019.01.005.

Kiriyama, E., Suzuki, A., 2004. Use of real options in nuclear power plant valuation in the presence of uncertainty with CO2 emission credit. J. Nucl. Sci. Technol. 41 (7), 756–764. Available at: https://doi.org/10.1080/18811248.2004.9715543.

Kirk, J., et al., 2025. Environmental impacts of decommissioning a nuclear power plant: a life cycle assessment of a Magnox site. Environ. Impact Assess. Rev. 113, 107880. Available at: https://doi.org/10.1016/j.eiar.2025.107880.

Kodukula, P., Papudesu, C., 2006. Project Valuation Using Real Options: A Practitioner's Guide. Ft. J. Ross Pub, Lauderdale, Fla.

Li, F.-F., Wang, Z.-Y., Qiu, J., 2019. Longterm streamflow forecasting using artificial neural network based on preprocessing technique. J. Forecast. 38 (3), 192–206.

Liu, Y.-W., et al., 2014. Drought assessment and uncertainty analysis for Dapoling basin. Nat. Hazards: J. Int. Soc. Prevent. Mitigat. Nat. Hazards 74 (3), 1613–1627.

Locatelli, G., et al., 2015. Load following with small modular reactors (SMR): a real options analysis. Energy 80, 41–54. Available at: https://doi.org/10.1016/j.energy.2014.11.040.

Locatelli, G., Mancini, M., Lotti, G., 2020. A simple-to-implement real options method for the energy sector. Energy 197, 117226. Available at: https://doi.org/10.1016/j.energy.2020.117226.

Marcel, C.P., 2023. Addressing the global energy problem: perspectives, challenges, and potential solutions. Nucl. Eng. Des. 414, 112610. Available at: https://doi.org/10.1016/j.nucengdes.2023.112610.

Middleton, B., et al., 2021. The Palo Verde water cycle model. SAND2021-5077C. Sandia National Lab. (SNL-NM), Albuquerque, NM (United States). https://doi.org/10.1115/POWER2021-65768.

Mombrini, E., et al., 2025. A 60-year drought analysis of meteorological data in the western Po River basin. Hydrol. Earth Syst. Sci. 29 (10), 2255–2273. Available at: https://doi.org/10.5194/hess-29-2255-2025.

Nalbantis, I., Tsakiris, G., 2009. Assessment of hydrological drought revisited. Water Resour. Manag. 23 (5), 881–897. Available at: https://doi.org/10.1007/s11269-008-9305-1.

de Neufville, R., Scholtes, S., 2011. Flexibility in Engineering Design. The MIT Press. https://doi.org/10.7551/mitpress/8292.001.0001.

Niu, W., et al., 2018. Forecasting daily runoff by extreme learning machine based on QuantumBehaved particle swarm optimization. J. Hydrol. Eng. 23 (3).

Nock, D., Baker, E., 2019. Holistic multi-criteria decision analysis evaluation of sustainable electric generation portfolios: New England case study. Appl. Energy 242, 655–673. Available at: https://doi.org/10.1016/j.apenergy.2019.03.019.

Noorbeh, P., Roozbahani, A., Moghaddam, H.K., 2020. Annual and monthly dam inflow prediction using Bayesian networks. Water Resour. Manag. 34 (9), 2933–2951.

Peachey, C. (2013) "An oasis filled with grey water - Nuclear Engineering International," Nuclear Engineering International, 25 June. Available at: https://www.neimagazine.com/advanced-reactorsfusion/an-oasis-filled-with-grey-water/ (Accessed: May 30, 2025).

Poinssot, Ch., Bourg, S., Boullis, B., 2016. Improving the nuclear energy sustainability by decreasing its environmental footprint. Guidelines from life cycle assessment simulations. Prog. Nucl. Energy 92, 234–241. Available at: https://doi.org/10.1016/j.pnucene.2015.10.012.

Pucciarelli, M., et al., 2024. Using life cycle assessment to quantify the environmental benefits of circular economy strategies in the nuclear industry. Prog. Nucl. Energy 168, 105026. Available at: https://doi.org/10.1016/j.pnucene.2023.105026.

Ramírez Molina, A.A., et al., 2024. Extraordinary 21st Century Drought in the Po River Basin (Italy). Hydrology 11 (12). https://doi.org/10.3390/hydrology11120219.

Raso, L., Chiavico, M., Dorchies, D., 2019. Optimal and centralized reservoir management for drought and flood protection on the upper Seine-Aube river system using stochastic dual dynamic programming. J. Water Resources Plan. Manag. 145 (3). https://doi.org/10.1061/(ASCE)WR.1943-5452.0001040.

Redfoot, E.K., McKellar, M.G., Borrelli, R.A., 2022. Allocating heat and electricity in an integrated energy system coupled with a water purification system. Nucl. Eng. Des. 397, 111902. Available at: https://doi.org/10.1016/j.nucengdes.2022.111902.

Riahi-Madvar, H., et al., 2021. Short to long-term forecasting of river flows by heuristic optimization algorithms hybridized with ANFIS. Water Resour. Manag. 35 (4), 1166.

Rossi, G., 2000. Drought mitigation measures: A comprehensive framework. In: Vogt, J. V., Somma, F. (Eds.), Drought and Drought Mitigation in Europe. Dordrecht: Springer Netherlands, Pp. 233–246. https://doi.org/10.1007/978-94-015-9472-1_18. Available at.

Rossi, L., et al., 2023. European Drought Risk Atlas. JRC Publications Repository. https://doi.org/10.2760/608737.

Russell, S., Moskowitz, I.S., Jalaian, B., 2020. Front matter. In: Human-Machine Shared Contexts. Elsevier, pp. 67–91.

Samui, P., et al., 2023. Comparison of different optimized machine learning algorithms for daily river flow forecasting. Earth Sci. Inf. 16 (1), 533–548.

Scarsini, S., Musolino, D., Massarutto, A., 2024. Every cloud has a silver lining: Winners and losers from droughts. J. Environ. Manag. 371. https://doi.org/10.1016/j.jenvman.2024.122954.

Sogin S.p.A., 2025. Caorso Nuclear Power Plant. Available at: https://www.sogin.it/it/chiusuradelciclonucleare/sitinucleariitaliani/centraledicaorso/Pagine/default.aspx (Accessed: November 2024).

Steer, S.J., et al., 2012. Minimising the economic cost and risk to accelerator-driven subcritical reactor technology: the case of designing for flexibility: part 1. Nucl. Eng. Des. 243, 135–147. Available at: https://doi.org/10.1016/j.nucengdes.2011.11.027.

UNECE, 2022. United Nations economic Commission for Europe. Carbon neutrality in the UNECE region: integrated life-cycle assessment of electricity sources. ECE Energy Series. United Nations [Preprint].

Wang, L., et al., 2019. A comparative life-cycle assessment of hydro-, nuclear and wind power: a China study. Appl. Energy 249, 37–45. Available at: https://doi.org/10.1016/j.apenergy.2019.04.099.

World Bank (2024) Glossary | DataBank. Available at: https://databank.worldbank.org/metadataglossary/world-development-indicators/series/EN.ATM.CO2E.EG.ZS (Accessed: September 18, 2024).

World Nuclear Association (2024a). Carbon Dioxide Emissions from Electricity, World-Nuclear.org. Available at: https://world-nuclear.org/information-library/energy-and-the-environment/carbon-dioxide-emissions-from-electricity (Accessed: May 29, 2025).

World Nuclear Association (2024b). World Nuclear Performance Report 2024. 2024/003. England: World Nuclear Association, pp. 1–33. Available at: https://world-nuclear.org/our-association/publications/world-nuclear-performance-report/global-nuclear-industry-performance-2023 (Accessed: May 29, 2025).

Zhang, W., Lin, Z., Liu, X., 2022. Shortterm offshore wind power forecasting - A hybrid model based on Discrete Wavelet Transform (DWT). In: Seasonal Autoregressive Integrated Moving Average (SARIMA), and deep-learning-based Long Short-Term Memory (LSTM). Renewable Energy, pp. 611–628.